Regulation of gene expression by RelA in activated B lymphocytes

By

Jaimy P. Joy

A dissertation submitted to Johns Hopkins University in conformity with the requirements for the degree of Doctor of Philosophy

Baltimore, Maryland

June, 2017

Abstract

B cells undergo dramatic alterations in response to antigen recognition through cell surface receptors, which requires active transcription and translation. The temporal expression of transcripts is germane and integral in determining underlying complex biological phenomena.

The transcription factor RelA is rapidly expressed in the nucleus in response to BCR crosslinking, and downregulated within hours. However, many putative NF-κB target genes expressed by stimulated B cells do not follow the same kinetic pattern as the transcription factor, suggesting complex transcriptional and post-transcriptional regulation. The current work seeks to explore the mechanisms by which genes are regulated by NF-κB in primary murine splenic B cells in response to BCR crosslinking. To do this, we examined the kinetics of genome-wide RelA binding, the inducible transcriptome, and RNA stability of induced genes.

NF-κB target genes, as inferred from RelA ChIP-seq analyses and pharmacological inhibition of IKK-2 inhibitors, were amongst the most highly induced genes in response to BCR crosslinking. Highly induced transcripts had shorter half-lives ($t_{1/2}$s) than those with less robust induction one hour after stimulation. The majority of inducible genes with fast $t_{1/2}$s displayed exponential decay, while the majority of inducible genes with slow $t_{1/2}$s displayed non-exponential decay.

As exponential decay is likely to mean a single-step decay mechanism and the 3' UTRs are known to play a critical role in RNA stability, we looked to the presence of RNABP consensus motifs in genes of various decay patterns. Our analyses revealed that hnRNPA1 binding sites were highly enriched in the 3' UTRs of genes with fast,

exponential decay. siRNA mediated knockdown of hnRNPA1 in two mature B cell lines, Bal17 and M12, revealed greater RNA stability of many genes that have fast, exponential decay and are RelA target genes based on inducible RelA binding and IKK-2 inhibition. These findings suggest a tantalizing model in which mRNA decay is dependent on transcription factors, such as RelA, that inducibly bind to its target genes and induce RNA.

Mentor: Ranjan Sen, Ph.D.

Reader: Joel Pomerantz, Ph.D.

Acknowledgements

The journey of 1,000 miles begins with a single step and I am grateful to have taken the first step five and a half years ago. It has been an arduous and tumultuous experience, but just as rewarding, and not one I would trade for anything. The science, friendships, and memories will be treasured for years to come.

To my friends and family who loved, supported, and encouraged me even when I didn't deserve it or show my appreciation for it, thank you. This body of work would have been impossible without your unwavering support. You no longer have to ask me "when will you be done?" and I no longer have to silently resent you for it.

To my thesis committee members, Joel, Stuart, and Jef, thank you for the consistent years of reliability and helpfulness. Your keen sense of good science and mentorship have been an invaluable part of my scientific growth and maturity. If only all grad students can be so lucky.

To the immunology training program, Mark, Joel, Ms. Angela, Ms. Lin, and Lori, thank you for giving me the opportunity to pursue my Ph.D.. You put up with a lot and I hope to make you proud.

To the members of the Sen lab, I could not have asked for a better group of people to call my work family. Everyone, both past and present members, has been an incredible resource and support system. If anyone goes through any of my lab notebooks and comes across random wrinkly patches and bleeding ink, assume I was having a bad day.

Finally, to Dr. Sen, the person I am lucky to have called my mentor, I (yes, even I) cannot fully express my gratitude due to the limited nature of the English language. I

came to Hopkins to be trained as a scientist and I leave knowing that to be true. From journal clubs, lab meetings, one-on-one meetings, seminars, to everything in between, I learned to question everything and be critical in my analyses. I could not have asked to train under a better scientist. Somehow, you also managed to be a good and patient person and set the bar for all PIs unrealistically high.

To any future graduate student who stumbles onto this thesis, it gets better, but if it doesn't, Robert Frost said it best: "it [life] goes on".

As this 1,000-mile journey ends, I wish to finish it in the same way I began, by giving thanks to Christ and trusting that the next one will be just as fulfilling.

Table of Contents

Table of Figures

Chapter I: NF-κB

Introduction: NF-κB

Since its discovery as an inducible protein bound to the intronic kappa light chain enhancer in activated B cells [1], RelA has been the focal point of research across several fields. Its ubiquitous nature makes it indispensable for development, survival, and programmed cell death (reviewed in [2]).

NF-κB and IκB family members

There are five members of the NF-κB family (RelA/p65, p105/p50, cRel, p100/p52, and RelB) that homo- or heterodimerize to provide combinatorial and functional versatility in biological systems (**Fig 1A**). These five family members are involved in either the canonical (RelA, p50, and cRel) or noncanonical (p52, RelB) pathway, which play largely non-redundant roles and have distinct functions in acute versus chronic cell responses, respectively (reviewed in [3]).

Each of the five NF-κB family members contains the hallmark Rel homology domain (RHD), which is necessary for DNA binding and dimerization. However, only RelA, RelB, and c-Rel contain transcription activation domains (TADs); neither p100 nor p105, contain TADs, which has led to speculation that these subunits act as repressors in homo- or heterodimeric forms, but this is likely not always the case as coactivators can be recruited to activate transcription. An essential component of NF-κB regulation is the family of inhibitor κB proteins (IκBs), made up of the typical members, IκBa, IκBb, and IκBe, the atypical members, IκBζ, IκBns, and Bcl-3, and the precursor proteins, p105 and p100 (**Fig 1B**). The IκB family members act to inhibit nuclear translocation and transcriptional activity of NF-κB proteins, which is accomplished largely by the ankyrin

repeat domains of IκBs binding to the RHD of the NF-κB subunits and masking their nuclear localization sequences [4].

NF-κB subunits and dimers have both unique and overlapping functions, as evidenced by the single and multi-family member genetic knockout mice. With the exception of *Rela*, genetic deletion of a single subunit does not result in a robust abnormal phenotype unless mice are challenged with infectious agents [5]. However, in the case of *nfkb1*$^{-/-}$ (encodes for p105), it has been shown that the average lifespan of the mice is reduced by approximately 50% [6].

NF-κB signaling

NF-κB family members are present in virtually all cell types and are activated in response to many different stimuli, although it is likely that the canonical pathway is also active at basal levels given the shuttling of NF-κB and IκB complexes between the nucleus and cytosol (reviewed in [7]). The canonical NF-κB pathway, which is dependent on IKKγ/NEMO, is active upon the stimulus-induced release of the NF-κB dimer from the cytoplasmic residing inhibitor, IκBα. Upon nuclear translocation, NF-κB binds to DNA resulting in both functional and nonfunctional consequences based on cell and stimulus type (**Fig 2**).

The canonical pathway is often activated within minutes in response to different stimuli, including TNFα, IL-1β, and LPS, resulting in the production of pro-inflammatory cytokines and chemokines across various cell types. Conversely, the noncanonical pathway, activated upon activation of CD40R, BAFFR, LTRβ, and other stimuli, is a slow response and more sustained relative to the canonical pathway (reviewed in [3]). Upon receptor engagement, the NF-κB inducing kinase (NIK) phosphorylates and

activates IKKα, which phosphorylates p100 and triggers the K-48-linked ubiquitination and subsequent proteasomal processing of p100 to p52. The RelB-p52 complex can then freely translocate to the nucleus and modulate gene expression (**Fig 2**).

Although the canonical and non-canonical NF-κB pathways are activated by different stimuli, lead to different signaling cascades, and give rise to different cellular responses, there is often crosstalk between the two pathways [8-10]. As cells are likely to be activated through multiple receptors at any given time in an *in vivo* setting, the two arms of NF-κB signaling are likely to be simultaneously active. It has even been proposed that the canonical and non-canonical pathways should be viewed as a single signaling system [11], but as each signaling pathway can function in the absence of the other, this may not be biologically practical.

Regulation of NF-κB

Dysregulated canonical NF-κB signaling is known to be associated with various cancers [12-14] and aging [15-17], which highlights the importance of a tightly controlled mechanism by which the pathway must be regulated. Thus, it is unsurprising that several regulatory mechanisms exist to limit NF-κB activation at different points in the signaling cascade as well as post nuclear translocation. Firstly, there are many combinatorial possibilities of homo- and hetero- dimers between the NF-κB family members which result in different outcomes depending on dimer composition. Since not all combinations are permissive to transcriptional activation, this is one way in which NF-κB activity can be limited (reviewed in [18]). Further, many target genes of the canonical NF-κB pathway are those that lead to a negative feedback loop, such as *Nfkbia* (encodes for IκBα) [19]. As a final example, although many more exist, NF-κB

subunits can be post-translationally modified, with some modifications being necessary for the transcriptional activation of target genes (reviewed in [20]).

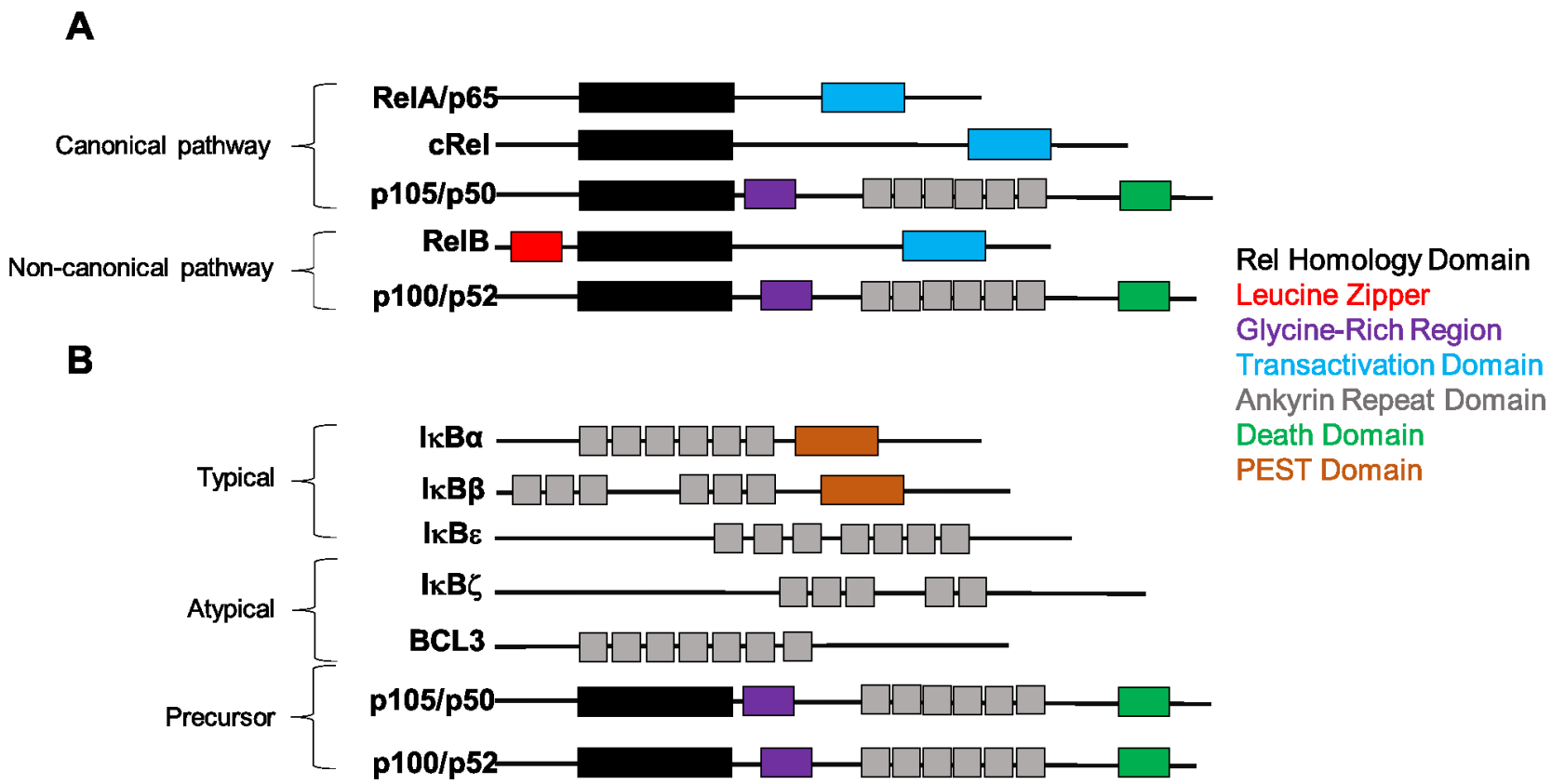

e 1. NF-κB and IκB family mem

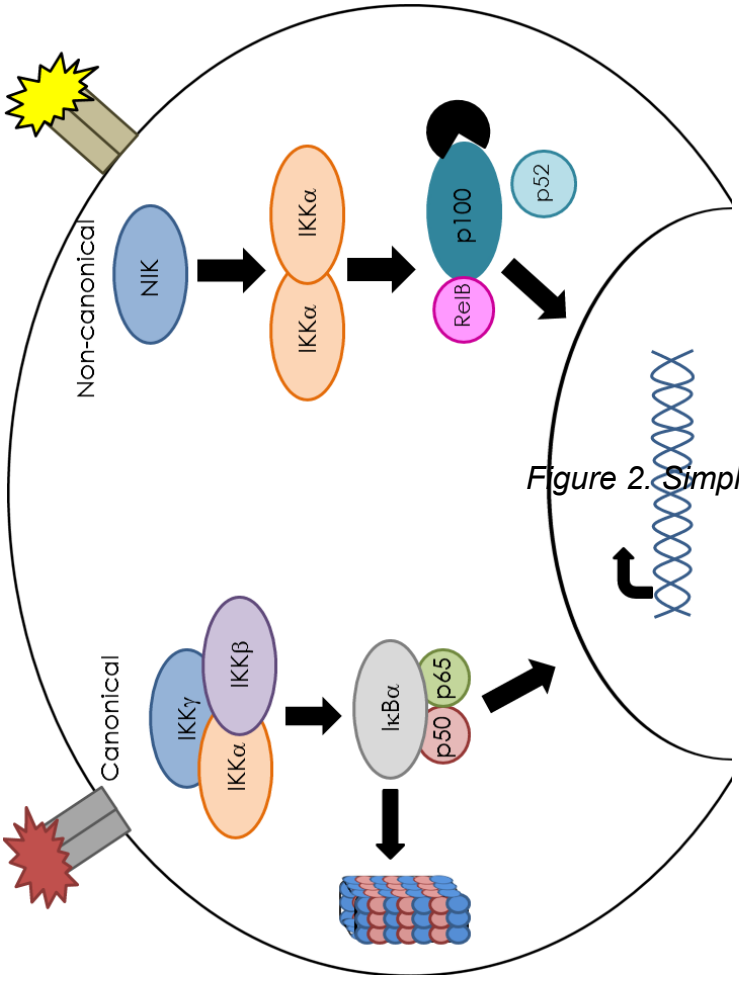

Figure 2. Simplified model of canonical and non-cano

NF-κB binding: specificity and dynamics

Surprisingly, several studies have provided evidence that most NF-κB target genes do not demonstrate dimer specificity [21-23]. Although early structural studies did not show evidence for sequence-specific NF-κB-DNA interactions [24, 25], crystal structures have since revealed that NF-κB dimers show some level of sequence specificity, but do not make contacts with the DNA at every nucleotide within the κB binding site. NF-κB dimers recognize κB sites through the Rel homology domain of each subunit, which mediates base-specific contacts through the DNA major groove to flanking (G)GG/(C)CC sequences within the loose consensus κB site, 5'-GGGRNWYYCC-3' [26]. This can therefore allow for a degree of "mobility" or alternative configurations, which also explains the compensation between family members. Given that dimer binding is inevitably linked to the ultimate functional output of a cell, one critical question in understanding RelA biology is the relationship between dimer binding site specificity and transcriptional output.

While the 5' and 3' GC-rich ends of the consensus κB site are mostly responsible for affinity and κB selectivity [27], central base pairs of the κB site may play an indirect role in binding specificity through regulation of the conformational state of the dimer [28]. RelA and c-Rel preferentially bind κB sites with AT-rich sequences in the center of the consensus κB binding motif, while p50 and p52 tolerate variability in the central bp sequence. In an *in vitro* system, the central bp in the κB site was found to play a role in the selectivity of dimer binding as well as its function. Using an ectopically expressed luciferase reporter in MEFs under the control of minimal promoter sequences, Wang et al found that a G/C centric κB site resulted in high luciferase activity in the presence of

p52 and Bcl3, but not RelA. In the case of an A/T centric κB site, however, luciferase activity is RelA dependent. These results indicate that under certain circumstances, dimer specificity is dictated by sequence specificity, which in this study, was solely due to the NF-κB binding site central bp. In addition to the recruitment of dimers that have distinct functions, the study went on to show that the DNA sequence may also influence the temporal order of some NF-κB target genes. RelA dimers were shown to mediate early induction whereas late expression was mediated by p52/Bcl3 based on mutational analysis of the central bp within promoters of known NF-κB target genes. Tip60, a HAT complex, was recruited to G/C centric κB sites within promoters of select genes, but not to A/T centric κB sites. Interestingly, though the p52/Bcl3 complex was recruited to an A/T centric site, HDAC3, a histone deacetylase, was recruited as a transcriptional repressor. Thus, the presence of one central bp over the other (A/T vs C/G) can influence which coactivators and corepressors are recruited and which genes will be induced early versus late [29].

Another example of sequence and dimer specificity playing a role in the regulation of NF-κB target genes is the case of IP-10, which is expressed in MEFs stimulated with TNF via the RelA/p50 heterodimer, but not the RelA homodimer. Despite both dimers showing similar *in vitro* binding affinities, a specific heterodimer is required for activation. However, MCP-1 gene expression under identical circumstances is activated by both dimers. This discrepancy between activation of the two genes is due to a single nucleotide difference in the κB binding site which determines coactivator recruitment; although the NF-κB dimer recruitment and binding was unaffected, the coactivator recruitment was altered [30]. This particular example, again, highlights how some

genes, under specific settings, are dependent on the DNA sequence, dimer composition, and coactivator recruitment. Yet another example of gene expression that is subunit-specific is IL-12 p40, which is selectively dependent on cRel as determined by analysis of cRel-/- macrophages. Interestingly, DNA binding and transfection assays showed comparable capacity for binding and transactivation between dimers with and without cRel, which highlights the importance of context-dependent regulation, especially in *in vivo* scenarios.

The previous studies looked to a small number of well-defined NF-κB targets, but it is highly unlikely that all target genes are regulated in the same manner. Owing largely to scientific and technological advances within the past decade, the field has begun to address the global dynamics of TF binding. Several genome-wide studies have shown that up to 90% of nuclear translocating TF (e.g. GR and NF-κB) binding sites are located in intra- and intergenic regions [22, 31, 32]. While not all of these sites may have functional consequences in a given cell type, the notion that TFs are critical in establishing enhancers and mediating transcription from a promoter distal perspective is now well accepted. For example, in macrophages stimulated with lipid A, RelA, in collaboration with other TFs, leads to stimulus-induced enhancer-like regions [33]. Papantonis et al demonstrated that HUVECs stimulated with TNF leads to discrete "NF-κB factories", which brings distal genes together in close enough proximity to co-regulate their expression [34]. Using Chromatin Interaction Analysis by Paired-End Tag Sequencing (ChIA-PET), Kuznetsova et al found that activation of GR and NF-κB in HeLa cells using triamcinolone acetonide and TNF led to long range chromatin contacts that linked enhancer "hubs" to target genes [35]. These studies, along with others,

demonstrate that RelA binding and activity extend beyond the simple role of transcriptional activation via promoter binding. This, of course, complicates the mechanistic dissection of the roles of RelA, but insights from several studies have made strong headway.

Many chromatin immunoprecipitation (ChIP)-chip and ChIP-seq studies have shown that a large proportion of sites to which RelA bind deviate considerably from the consensus motif. One of the first studies to conclude that RelA binding cannot be equated to gene activation showed that there was a high enrichment for GATA-3 and CRE-BP binding motifs after RelA ChIP-seq [36]. In an early study using ChIP-chip with each of the five NF-κB family members, Richard Young and colleagues found that the majority of induced RelA binding events in a monocytic cell line stimulated with LPS occurred at promoters of target genes that were already occupied by p50 in the unstimulated state [23]. Although no motif analysis was carried out, they concluded that induced RelA binding that joins pre-existing p50 is not exclusively dependent on the presence of the κB consensus motif. Lim et al used ChIP-PET and showed that less than half of RelA-bound loci contained consensus RelA binding motifs [21]. Other RelA ChIP-seq studies consistently report only 50-70% of RelA binding to consensus κB sites [37]. The fact that motifs other than that of RelA are being enriched is likely reflective of binding/interacting with other TF complexes.

In a systematic approach to elucidate NF-κB dimer specificity exclusively at the DNA sequence level, Siggers et al used protein-binding microarrays and surface plasmon resonance to determine binding affinities. They found that various NF-κB heterodimers show highly similar binding specificities and may, therefore, regulate gene expression

primarily through dimer-specific interactions instead of sequence specificity alone [38]. A more recent study used RelA ChIP-seq and predictive RelA motifs and showed an enrichment of genes whose promoters combined strong ChIP-seq peaks and NF-κB motifs among strongly induced primary response genes (PRGs) in lipid A stimulated BMDMs [39]. Of the PRGs that had high RelA motif scores, based on PBM scores using an artificial p65/p50 heterodimer, approximately 85% of them show strong promoter binding as measured by p65 ChIP-seq peak intensity. The results of this study, as well as our own, highlight the value of high throughput data analysis by categorizing genes based on strength of TF binding, the genomic and epigenomic landscape (discussed in upcoming sections), and gene expression. Despite many genomic binding events, RelA binding to a select number of critical PRGs in response to a specific stimulus is dependent on the presence of a strong NF-κB consensus motif. Further, the number of NF-κB motifs did not correlate either with the strength of binding based on p65 ChIP-seq or transcriptional induction based on RNA-seq. The authors of this study concluded that at the promoters of most PRGs in BMDMs, a strong RelA consensus motif almost always supports strong RelA binding.

NF-κB binding, based on many RelA ChIP-seq experiments across several cell types, is widespread across the genome in response to an inducing stimulus. Sequence and dimer specificity are known to be vital in specific instances, but genome-wide studies suggest that most RelA binding is not limited to the consensus κB motif and in the absence of one family member, there is compensation between subunits. While not all binding leads to a functional output in terms of transcription, other outcomes, such as mediating long-range interactions, are possible. The following sections highlight our

knowledge of productive RelA binding, that is, binding that results in transcription, and the factors that dictate productive vs nonproductive binding.

Cell and stimulus-specific activation of NF-κB

Many different stimuli induce an NF-kB response, but the functional output of the cell (i.e. transcription) varies based on the cell- and stimulus-type. Many different stimuli, including TNFα, IL1β, and reactive oxygen species (ROS) are known to activate the canonical NF-κB pathway, but despite inducing the same family of transcription factors, the cellular response is dramatically different. Depending on the cell- and stimulus- type, the kinetics of NF-κB nuclear translocation, the dimer compositions, and interaction with other TFs and cofactors vary. The mechanisms by which this specificity is achieved remain somewhat elusive, although many studies have attempted to address this.

Chromatin accessibility and histone modifications

Selectivity of the NF-κB response is accomplished through multiple layers of regulation [18] with cell-specific chromatin landscapes playing an integral role in the cell-specific functions of NF-κB. Tissue-restricted DNase I hypersensitive sites, for example, are often more amenable to rapid TF binding and subsequent transcription of target genes unique to a cell type [40]. Studies have shown that *de novo* binding of nuclear translocating TFs after stimulation to the genome occurs largely at DNase I hypersensitive sites, or pre-existing chromatin accessible regions [41-43]. However, a meta-analysis correlating DHS-seq and RelA ChIP-seq across various cell types found approximately 32% of all induced RelA peaks outside of DHS sites [37]. To this point, histone modifications also influence NF-κB activity and the coordination of various histone marks in combination with DNAse I hypersensitive sites can provide insights into TF binding and gene regulation. DNAse I hypersensitive, enhancer-like sites that recruit RelA have higher levels of many histone modifications, but most notably

H3K4me1. Motif based prediction of inducible RelA binding was significantly improved when looking to sites that have a histone modification in the uninduced state. RelA binding is also influenced by the DNA methylation status (both promoter-proximal and distal); hypomethylated CGI sites had increased RelA binding while methylated CGIs showed no TF enrichment, especially at promoter-proximal sites. Based on the meta-analysis, H3K4me1 and H2A.Z status are associated with p65 binding at enhancers and promoters; in fact, the dual presence of both modifications was found to be the strongest predictor of RelA binding to enhancers. Interestingly, the co-occurrence H3K27me3 and H2A.Z has the opposite effect and showed very little enrichment for RelA binding. Within the same meta-analysis, Although the correlation between RelA binding and the presence of other TFs was less robust than with histone modifications, the authors concluded that site-specific RelA binding is possibly guided by the presence of particular TFs, such as GATA3, BCL3, and CREB1, which may or may not be cell-specific. Thus, the chromatin landscape, not only in terms of histone modifications and accessibility, but also pre-bound cell specific TFs, plays a critical role in the RelA binding patterns seen across cell types. [37].

Much work has been done in various cell types stimulated with inflammatory stimuli, such as TNF, which in turn leads to the production of NF-κB dependent pro-inflammatory cytokines and factors [40, 44, 45]. In a recent study, investigators looked to the immediate effects of TNF stimulation on nucleosome positioning, using MNase-seq, in HUVECs. As early as ten minutes after stimulation, nucleosome repositioning occurs, with the newly unmasked regions showing motif enrichment for proinflammatory TFs, especially NF-κB. RelA ChIP-seq revealed that there was minimal inducible RelA

binding at ten minutes, but binding was highly upregulated at 30 minutes. In the case of *NFKBIA*, the best characterized true and direct target of p65 (reviewed in [18]), nucleosome repositioning occurred at ten minutes, but peaked at 30 minutes followed by RelA binding at the promoter. Thus, in HUVECs, and possibly in other cell types stimulated with an inflammatory agent, nucleosome positioning occurs independently of NF-κB binding and elongating PolII. The authors put forth an intriguing conclusion that NF-κB binding is a very selective process, with the initial binding events occurring in primed domains that are depleted of nucleosomes and contain high affinity binding sites (i.e. minimal deviation from the consensus sequence) [46]. It was not clear, however, what mechanisms dictate the repositioning of nucleosomes to expose the high affinity NF-κB binding sites.

TF and cofactor interaction

Another mechanism by which NF-κB maintains both cell- and stimulus- specificity is via interactions with cofactors and/or other TFs that are specific to a cell-type or are induced in response to a particular stimulus. It has been previously demonstrated that the phosphorylation of serine 276 of RelA allows for interaction with CBP/p300, a transcriptional coactivator, to activate gene expression for a subset of target genes. To more thoroughly investigate genes that that are dependent on this interaction, Mukherjee et al expressed RelA mutants in RelA-/- fibroblasts that disrupt interaction with CBP/p300. They found that CBP/p300 was preloaded on promoter regions of a subset of RelA target promoter regions, which supports the conclusion that RelA may be recruited to its target sites by the coactivator complex [47]. Surprisingly, NFKBIA and TNFAIP3 (encodes A20) were among the genes whose expression was dependent on

RelA interaction with CBP/p300, despite a previous report that concluded otherwise [48]. Thus, subunit-specific modifications and specific coactivators and TFs are critical determinants of cell-and stimulus-specific NF-κB responses.

The ubiquitous nature of NF-κB family members requires tight regulation across cell types and in response to certain stimuli to elicit the appropriate response. Cell specificity is largely accomplished by the chromatin landscape, other cell-specific TFs, and variable kinetic patterns of NF-κB. Stimulus specificity can also be achieved by myriad possibilities, including interactions with coactivators or corepressors that are simultaneously activated or recruited, and activation of specific NF-κB subunits in response to unique stimuli.

NF-κB dependent transcription and target genes

Existing NF-κB target gene databases

For more than two decades, several notable attempts to identify and catalog NF-κB target genes have been made, but are likely overestimations of the actual number of direct targets. Currently, many curated lists of putative NF-κB target genes are available online (http://www.bu.edu/nf-κB/gene-resources/target-genes/, http://bioinfo.lifl.fr/NF-KB/, and http://tfdb.seu.edu.cn/nfκB/). These genes, however, are largely deemed NF-κB targets based on luciferase reporter assays using minimal promoter sequence sequences. While informative, context dependent NF-κB regulation and non-promoter related regulation are not taken into account. The most recently generated database of NF-κB target genes by Yang et al was based on studies that, at a minimum, used NF-κB ChIP to define target genes. A useful feature of this database is that for each gene, the cell type, inducing stimulus, and other details about the system in which the target gene was determined, is provided. Again, however, this compilation of genes, which is currently approximately 2,300 in number, is likely to be an overestimation of NF-κB target genes.

Criteria for NF-κB target gene identification

Based on earlier technologies and techniques, it was postulated that in order to establish that a gene is truly regulated by NF-κB, binding to a putative DNA site must be demonstrated by EMSA, the regulatory region (e.g. promoter and/or enhancer) must show transcriptional activity using an *in vitro* reporter assay, and mutagenesis of the putative binding motif should abolish binding [19]. With a better understanding of TF biology and the availability of more sophisticated techniques, however, we now know

that these criteria alone do not accurately classify a gene as a true NF-κB target gene. It has been previously demonstrated that EMSA-based binding may not have functional consequences [49] and use of cell extracts in *in vitro* assays can be misleading as they may contain other TFs and cofactors that can promote cooperative binding. Instead, genetic ablation and/or pharmacological inhibition of NF-κB coupled with mutational analyses of putative TF binding sites are needed to label genes as direct targets of the TF. Further, identification of a target gene also requires evidence of transcriptional output, which can be measured via RNA-seq, qPCR, RNA FISH, and other methods. Thus, while many RelA ChIP-seq experiments exist in the literature, RelA binding alone does not indicate the transcriptional status of a gene; RelA ChIP-seq coupled with RNA-seq has become a standard measure of identifying target genes, but this, too, is insufficient in the absence of functional follow-up studies. Functional studies can include, but are not limited to, a comparison of gene expression profiles in wildtype vs knockout cells, pharmacological inhibition, and/or overexpression studies, although the latter is less straightforward. These measures are necessary to both confirm functional binding, but also to determine distal binding sites (enhancers) in the regulation of target genes.

Experimental determination of NF-κB target genes

In an early study that aimed to identify RelA target genes in HeLa cells stimulated with TNFα, Zhou et al performed siRNA knockdown of RelA followed by cDNA microarray. 16 genes whose expression was inhibited by RelA knockdown compared to control knockdown were validated by qPCR after which promoters of these genes were scanned for NF-κB binding motifs. At least one NF-κB binding motif was found within 3

κB upstream of the transcriptional start site in almost all genes, but these sites were not followed up with functional analyses [50]. A more comprehensive study came from Tian et al, which sought to systematically identify NF-κB target genes in fibroblasts stimulated with TNFα [51]. To this end, a dominant negative IκBα was expressed under the control of an inducible tetracycline system in HeLa cells. Cells were stimulated for 1,3, or 6 hours in the presence or absence of doxycycline to identify target genes of the canonical NF-κB pathway followed by microarray. TNFα-regulated NF-κB independent genes were involved in metabolism, signaling, and encoded for other transcription factors and immediate-early genes. Approximately 30 genes were identified as TNFα-regulated NF-κB-dependent genes and encoded for cytokines/growth factors and factors involved in TNF signaling and regulation of NF-κB signaling. To determine if overexpression of RelA was sufficient to activate these NF-κB dependent genes, EGFP-RelA was ectopically and transiently expressed in HeLa cells. Of 12 representative NF-κB target genes, 10 were activated with RelA overexpression, although induction magnitude was much less than with TNF stimulation.

To further bolster the status of these genes as NF-κB-dependent, putative NF-κB binding sites were verified by EMSA. For a small subset of these genes, the authors looked to RelA recruitment to their promoters and found RelA enrichment under normal conditions, but not in the absence of doxycycline, i.e. when canonical NF-κB signaling is inhibited. While this study was very thorough in terms of the measures needed for the identification of *bona fide* RelA target genes, there were less than a dozen genes that emerged as true NF-κB targets, potentially by virtue of the few number of genes that were pursued following microarray. Nonetheless, this study was the first to apply

systematic approaches to identifying NF-κB target genes and newly identified RelA target genes, such as nuclear assembly factor 1 ribonucleoprotein, *Naf1*.

Monophasic vs oscillatory NF-κB activity

Another complication in the pursuit for real NF-κB target genes is the variability of nuclear NF-κB levels and translocation between single cells in a population, which translates to differential NF-κB-dependent gene expression patterns. Early single cell imaging experiments revealed that TNF stimulation in fibroblasts leads to both monophasic and oscillatory modes of NF-κB activation patterns [52]. Since then, many follow-up studies have shown differential NF-κB kinetics between single cells in a population [53, 54]. In a follow-up study, the same group addressed whether the oscillatory pattern of NF-κB activation in fibroblasts treated with TNFα leads to distinct and unique genetic programs which activate different target genes at each oscillation. Kinetic analyses were performed on datasets generated in [51] and NF-κB dependent genes were categorized as early, middle, late, or biphasic, based on peak RNA expression time. Promoter regions of early and late response genes were analyzed by TRANSFAC to find potential regulatory features that dictate temporal gene expression. The number and location of consensus NF-κB binding motifs and location of AP-1 binding sites were comparable between early and late genes, but they found that the presence of NF-κB binding sites in phylogenetically conserved regions was unique to early genes. The authors suggested that early gene promoters were under a greater selective pressure than late genes to preserve high affinity NF-κB binding sites. Although further analysis is warranted to determine if this is true, current evidence supports this hypothesis as many of the genes defined as early in this study are

cytokines and chemokines that are activated in many different cell types by NF-κB, while the late genes are more cell- and stimulus-specific.

Single cell analyses in the pursuit of NF-κB target genes

Although it is not the only determinant, nuclear levels of RelA directly influence transcription of its target genes. Importantly, however, the presence of nuclear RelA does not correlate with gene expression of target genes. To this point, Nelson et al used fluorescence imaging of RelA and IκBa together with luminescence imaging of NF-κB dependent transcription (TNFα) and found that nuclear translocation of RelA is not sufficient for continuous TNFα transcription, as its transient nature is maintained in response to stimulus [55].

In a recent study, Lee et al. used immunofluorescence and RNA-FISH to measure eGFP-RelA nuclear translocation and transcription of early response genes, respectively. Dual labelling of the TF and three different target genes allowed for monitoring the direct relationship between these two events at the single cell level. In response to TNF stimulation, HeLa cells that were stably transfected with eGFP-RelA showed varying levels of nuclear RelA translocation from cell to cell. smFISH probes for three NF-κB dependent genes, IL8, NFKBIA, and TNFAIP3, were used as transcriptional readouts. Using a series of descriptors, it was found that the maximum fold change of nuclear eGFP-RelA was the strongest predictor of mRNA output. The study went on to mechanistically explain how cells can detect a pre-ligand state to ultimately sense a fold change in the nuclear RelA levels and proposed an indirect inhibitory pathway model [53]. The findings of this study were intriguing as it proposed how cells can tolerate cell-to-cell variability of NF-kB abundance and activity.

Kinetics of NF-κB target genes

As we have previously reviewed [18], three major parameters define the kinetics of NF-κB dependent genes: rate of gene induction, the duration of functional promoter-bound complexes, and the rate of mRNA degradation.

Rate of gene induction

The rate of gene induction is dependent on several factors, the most important ones being promoter architecture of RelA target genes and nuclear levels of RelA. Promoter architecture includes, but is not limited by, the number of NF-κB motifs, the presence and proximity of binding sites for other TFs relative to NF-κB motifs, nucleosome occlusion, and the chromatin landscape. While some studies have suggested that the number of NF-κB motifs is associated with higher levels of gene expression [23], others have found little correlation [39]. This, of course, can be directly impacted by interplay with other TFs that may either positively or negatively regulate transcription initiation. It is important to note, however, that promoter dependent RelA binding alone is not sufficient to delineate the role of the TF in transcription initiation. Considering that the genomic landscape of both promoters and enhancers that leads to transcriptional initiation is very similar [56] and a significant proportion of RelA binding occurs at enhancers, it is conceivable that enhancer binding plays a critical role in RelA dependent transcription. As reviewed in [57], the chromatin landscape is a critical determinant of NF-κB dependent gene regulation. In a previously mentioned study that used ChIA-PET to investigate how GR and NF-κB regulate their target gene repertoire from distal binding sites, RelA binding occurred at distal genomic loci, about 90% of which contained pre-bound p300, while a small fraction of genes showed both inducible

RelA and p300 binding. Induced and pre-existing p300 peaks that overlapped with RelA were enriched for NF-κB response elements (NREs) or AP-1 motifs, respectively. Overall, the authors found that GR and p65 mostly join pre-existing enhancer-like p300 distal binding sites that are set up by other TFs, such as AP-1. Based on this and other studies, RelA mostly bind to pre-existing “open” chromatin, at least during early timepoints after stimulation, but it remains unclear whether the TF binding creates accessible regions at later timepoints after activation. To relate chromatin state to transcriptional regulation, the authors used PolII density along the gene body as a proxy for gene expression. Using this measure, they found that genes with induced p300 and RelA are more highly expressed than those that are preexisting. These findings suggest that robust transcription of target genes, at least in part, is due to *de novo* binding of TFs and cofactors.

Duration of functional promoter-bound complexes

The second criteria used to define NF-κB target gene kinetics, duration of functional promoter-bound complexes, is the least studied aspect of the three parameters. To effectively study functional promoter-bound complexes, the promoter element to which RelA binds, RelA itself, and the transcriptional output of the target gene, must be considered. It is challenging to incorporate all of these conditions in a single model system that effectively recapitulates *in vivo* events. RelA-dependent transcription is a function of active NF-κB dimers bound to a target gene promoter (or any regulatory element). To date, few studies have directly addressed the factors involved in functionally active promoter bound complexes and the mechanisms involved in dissociating active complexes to turn off transcription. It is possible that NF-κB subunits

are substituted to cease transcription, such that subunits with TADs are replaced with those that lack them. Recent studies have provided evidence that transcription alone is not sufficient to define the kinetics of NF-κB target genes as splicing also plays a major role in the mature transcript output, discussed in greater detail below [58, 59].

Rate of mRNA degradation

The final parameter for NF-κB target gene kinetics, the rate of mRNA degradation, is an essential piece of the NF-κB puzzle. Apart from the dissociation of functional promoter/enhancer complexes, leading to a halt in transcription, there is considerable post-transcriptional regulation that determines mRNA lifetimes. A study by Hao and Baltimore in 2009 sought to mechanistically determine the factors that dictate the temporal expression of inflammatory genes in mouse fibroblasts [60]. Genes activated via TNF stimulation in fibroblasts were grouped into three categories based on early, intermediate, or late induction kinetics. mRNA stability was measured using actinomycin D within each induction category, which revealed distinct patterns of decay. The early induced genes were rapidly degraded, the intermediate induced genes had longer half-lives, and the late induced genes had even greater stability. The investigators went on to perform promoter-3' UTR swapping experiments between genes of different kinetic patterns and concluded that the 3' UTRs were the major determinant of gene expression patterns, largely due to the presence of AU-rich elements (AREs). This study provided evidence of temporal expression of genes activated in response to an inflammatory stimulus being encoded within the genome via the 3' UTR. However, the fact that the transcription induction kinetics were very variable (up to 10-fold) based on the promoter was not addressed. In a later study by the same group, it was proposed

that the timing of gene transcription is directly controlled by the intracellular concentration of NF-κB, but mRNA production lags the transcription kinetics [58]. To test this, RNA was collected from BMDMs minutes after stimulation with TNF and subjected to qPCR with primers to test for pre-mRNA and mature RNA. Despite the induction times and expression patterns of mature mRNA, the levels of pre-mRNA are rapidly induced across the three groups. Actinomycin D treatment soon after TNF stimulation revealed a decrease in unspliced transcripts accompanied by an increase in the corresponding spliced transcripts, which is in agreement with a model whereby mRNA kinetics are determined by splicing and not by transcriptional induction. Another study came to a similar conclusion using chromatin-associated RNA from bone-marrow derived macrophages; after stimulation with LPS, they found an accumulation of unspliced transcripts, contrary to the commonly held view of co-transcriptional splicing [61]. Splicing alone, however, does not account for the precise timing of NF-κB target genes as there are highly variable times of mRNA output and many genes whose induction is dependent on chromatin remodeling.

Outstanding questions

Many, but not all, target genes of NF-κB are not solely dependent on a single family member or dimer for expression. Redundancy and/or compensation between NF-κB family members have been reported in various model systems. For example, cRel, which is largely expressed in hematopoietic cells, is virtually undetectable at the protein level in MEFs, but is highly expressed with the knockdown of RelA (unpublished observations). This apparent increase in cRel recapitulates much of the functional binding of RelA, but it is less clear to what extent this change, if any, in dimer composition affects transcription and mRNA levels. While it is clear that certain genes are solely dependent on one subunit or the other [49], the majority can be compensated, but the consequences of subunit alternation are understudied.
Another open question is the dwell time or the time during which RelA remains bound to the DNA to influence gene expression. This, of course, would be best investigated at the single cell level and requires high resolution visualization of tagged RelA. We speculate that dwell times vary based on the sequence to which the dimer binds, which in turn, affects the regulation of gene expression. Another related question is the relative contribution of binding site affinity and avidity; the threshold of the amount of RelA (molecules of TF) for functional activity may vary across the genome based on the site to which it binds. Stronger motifs may require less RelA while weaker motifs may require more, but this is still an open question. Related to this, it is conceivable that a less stringent binding motif (i.e. deviations from the RelA consensus) can be compensated by increased recruitment of NF-κB. Studies have suggested that increased binding (avidity) supports high levels of mRNA expression [23], but this

requires further experimentation. Further, the lack of strong binding motifs may allow for more levels of regulation in terms of interplay with other TFs.

B cell biology

B cell development and B cell subsets

The adaptive arm of the immune system is comprised of T and B lymphocytes and is necessary for pathogen-specificity and immunological memory. Hematopoietic stem cells (HSCs) differentiate into multipotent progenitor cells, followed by common lymphoid progenitor cells, which subsequently gives rise to B, T, and NK cells. While precursor cells migrate to the thymus to develop into T cells, B and NK cells develop in the bone marrow (reviewed in [62]). Through a series of stage-specific gene expression patterns and gene rearrangements that provide antibody specificity, B cells develop to near maturity and exit the bone marrow to complete development in the spleen. Once in the spleen, B cells differentiate into follicular or marginal zone B cells. Follicular B cells are $IgM^{low}IgD^{hi}CD21^{med}CD23^{+}CD1d^{low}$ and can freely circulate in the periphery while marginal zone B cells are $IgM^{hi}IgD^{low}CD21^{hi}CD23^{-}CD1d^{hi}$ and restricted to the marginal zone of the spleen [63]. Functionally, follicular B cells are important for T-cell dependent immune responses, while marginal B cells are activated in a T-cell independent manner.

Epigenetic landscape of B cells

Cumulative efforts from studies looking to the epigenetic landscape of mature naïve and activated B cells have offered considerable insights into B cell biology. Choukrallah et al investigated the enhancer landscape and dynamics during B cell differentiation from HSCs to pro-B cells to mature splenic B cells. Using ChIP-seq analyses of various histone modifications that identify enhancer states, the investigators compared the epigenetic profiles of each cell type and found that the enhancer landscape is dynamically reshaped during B cell differentiation. They reported approximately 40,000

enhancers in HSCs, while pro-B and mature B cells each had around 25,000. Surprisingly, most active enhancers in mature B cells (H3K4me1, H3K27ac, active transcription) were not primed (H3K4me1) in the previous stages (HSCs and pro-B) and were established exclusively in the stage in which they played a role. Mature, LPS-activated B cell-specific enhancers were enriched for binding motifs of Oct2, NF-κB and IRF1/2/ 4. The enhancer landscape of resting mature B cells, however, remains to be determined, and is likely very different from activated cells as activation and plasma cell differentiation is known to induce dramatic modifications across the epigenetic landscape [64].

Critical to B cell responses after antigen encounter is the gene expression pattern tailored to mounting an effective immune response. Early transcriptional landscapes that lead to different fates after B cell activation have been reported to emerge as early as two hours after stimulation [65]. In this study, it was reported that there was a genome wide increase of PolII at the TSSs of both uninduced and induced genes two hours after BCR stimulation while TLR4 stimulation led to a more robust transition from PolII initiation to elongation. While this is one interpretation of the data, initiating vs elongating PolII was defined on the sole basis of the genomic location to which PolII was bound; PolII bound to regions downstream of TSSs were deemed elongating, but this may be due to PolII recruitment. That additional genome-wide PolII recruitment occurs at the TSSs in response to BCR stimulation possibly allows for more robust and more rapid transcription of genes. Transcriptome analysis of BCR and TLR4 stimulated B cells revealed a Myc signature 2 hours after BCR stimulation and an NF-κB signature after LPS stimulation. In a study that sought to delineate the role poised PolII in B cells,

Dao et al compared PolII profiles in B cells that are resting and activated (72 hours after LPS treatment). Genes that were defined as having poised PolII in both resting and activated B cells wereκ enriched for gene ontologies that were non-B cell specific, such as DNA replication and apoptosis. Conversely, genes that were defined as non-poised in activated cells were enriched for gene ontologies such as lymphocyte activation, which the authors called “B cell specific”. It should be noted, however, that poised vs non-poised was defined as the relative levels of PolII in the promoter normalized to the gene body; thus many genes that were poised in resting, but non-poised in activated, B cells, were defined as such due to active transcription, which was verified by transcriptome analysis. Immediate early genes such as *Jun, Fos,* and *Egr1* were non-poised and highly expressed in resting B cells, but poised and lowly expressed in activated B cells. The authors concluded that in some instances, PolII poising accompanies attenuation of expression of previously active genes. Taken together, transcription of RelA target genes is a highly coordinated system that is influenced by a myriad of context-dependent factors, including histone marks, PolII, and other TFs.

NF-κB in B cells

Several groups have demonstrated that both the canonical and non-canonical NF-κB pathways are important in B cell generation, maturation, and/or maintenance (reviewed in [66]). Mature B cell survival is dependent on both the B cell receptor (BCR) and BAFF-R, the former of which activates the canonical NF-κB pathway while the latter activates the noncanonical pathway (reviewed in [67]). Absence of either the BAFF-R or BAFF results in the loss of virtually all mature B cells [68, 69]. Likewise, conditional deletion of genes leading to the disruption of the BCR complex led to the loss of mature B cells within 48 hours [70, 71]. Constitutive PI3K, but not IKK2, activity rescues peripheral B cell survival in absence of the BCR, which indicates that NF-κB signaling alone cannot confer survival signals in mature B cells.

Conditional deletion of IKKβ in B cells results in almost half the number of mature B cells although immature B cell numbers are unaffected [72]. IKKβ-/- B cells cultured *in vitro* undergo increased apoptosis and impaired response to various stimuli, including LPS, CD40, and IgM. These results strongly suggest that the IKKβ dependent canonical NF-κB signaling pathway plays a vital role in resting mature B cells, at least in part by positively regulating the synthesis of anti-apoptotic proteins [72, 73]. IKKa is required for optimal B cell maturation as IKKa-/- fetal liver derived B cells do not mature past the transitional T2 stage. B cells from IKKaa/a mice, which contain S→A mutations at positions 176 and 180, thus preventing phosphorylation, reach maturity, but have a dramatic reduction in the number of mature B cells in secondary lymphoid organs [74, 75].

Conditional deletion of cRel and RelA in GC B cells (loxP-RelA and loxP-cRel mice crossed to Cg1-Cre) led to the finding that cRel, but not RelA, is necessary for maintenance of the GC reaction. However, plasma cell differentiation was affected by deletion of RelA. B cells activated with anti-IgM leads to the rapid upregulation of RelA, followed by the slow and sustained upregulation of cRel. To investigate the B cell-intrinsic functions of RelA and cRel during B cell activation, Milanovic et al used conditional knockouts of RelA and/or cRel. Percentages of splenic B cells in both single KOs were comparable with WT, while the double deletion resulted in a dramatic reduction.

B cells stimulated with the F(ab')2 fragment of IgM leads to BCR crosslinking and rapid NF-κB nuclear translocation [76]. After the initial wave of RelA, *de novo* cRel accumulates up to approximately 24 hours after initial stimulation. Though experimental evidence is lacking, it is likely that the first phase of NF-κB (RelA dependent) is necessary for the rapid production of cytokines, chemokines, and growth factors needed to mount an effective immune response *in vivo* while the second phase (cRel dependent) is likely necessary for B cell survival and proliferation [77, 78]. Interestingly, the second phase does not seem to be either a direct or indirect consequence of RelA based on unperturbed cRel kinetics after treatment with IKK-2 inhibitors or in PKC-beta-/- B cells, which impairs the first phase of NF-κB (unpublished). Despite its critical roles in B cell gene expression, the RelA-dependent transcriptional program has not yet been delineated, which is the aim of this body of work.

Project Goals

In response to antigen recognition through cell surface receptors, B cells undergo dramatic alterations to break out of their naïve state, which requires active transcription and translation. The temporal expression of transcripts is germane and integral in determining the cellular response. From a molecular and cellular perspective, transcription factor binding and transcript expression is key to a better understanding of how cells respond to stimuli that ultimately lead to different fates and phenotypes. This work seeks to explore RelA/p65-dependent gene expression and identify RelA targets in response to BCR crosslinking.

The specific aims of this work are to:

1. Determine kinetics of transcription in B cells treated with αIgM.
2. Identify genome-wide binding sites and determine kinetics of RelA following BCR crosslinking in primary murine B lymphocytes.
3. Calculate half-lives of transcripts using high-throughput mRNA expression data.
4. Connect RelA binding, transcription, and RNA stability to comprehensively determine the RelA response of B lymphocytes.

Chapter II: BCR-induced NF-κB response in B cells

Kinetics of transcriptional response to BCR stimulation

In response to BCR activation, gene expression is widely altered; therefore, we chose to systematically dissect the biology underlying these complex phenomena. We performed RNA-seq across a six hour time course in B cells stimulated with αIgM. The data was processed and normalized using the Tuxedo Suite pipeline and RPKM cutoff was set at 1.5. Genes were grouped into six patterns based on kinetic profiles using k-means clustering (**Fig 3A**). The largest number of genes (roughly 3000) was in category I, in which gene expression peaked at four hours after stimulation, while the fewest number of genes (roughly 1000) was in category III, in which gene expression peaked at one hour and quickly returned to baseline. That half of the transcriptome clusters (I, II, and III) represent induced gene expression reflects the dramatic and rapid changes that occur in response to stimulation. Cluster VI represents a subset of genes that are inducibly downregulated, which may offer insight into the transcriptional program needed to maintain quiescence, but is outside the scope of this work. Gene ontology analysis of each transcriptome cluster revealed that there is an enrichment for “signaling by interleukins”, “NF-κB signaling pathway”, and “cytokine signaling in immune system” among genes in cluster III (**Fig 3B**). Indeed, many of the genes that were induced within the first hour after BCR activation are chemokines and cytokines, which are important for an optimal B cell response during antigen encounter *in vivo*. *Tnf*, *Ccl3*, and *Ccl4*, for example, are critical for promoting expansion and recruiting T cells and are represented in cluster III of our analysis [79, 80].

Since clustering induced genes in a single category may inadvertently lends bias towards lesser induced genes [39], we approached our RNA analyses from the perspective of both modest (<100) and robust (≥100) fold change. When we looked to RNA fold change at the peak time of expression within each cluster, approximately 10% of genes from clusters II and III showed a robust fold change in RNA expression, while clusters I and IV had less than 5% of genes with this level of induction. Since peak expression time of genes in clusters V and VI occur at baseline, fold change is not applicable in this respect. It should be noted that the magnitude of fold change within each cluster did not necessarily correspond to RPKM values (**Fig 3C**). As different genes have different requirements for expression, it is conceivable that in some cases, absolute levels of RNA are the key determinant, while in other cases, fold change may be more reflective of functional biological consequences. Our analyses have attempted to take into consideration both RPKM and fold change of RNA to include all genes that are likely to be biologically important. Stimulus-induced genes that rapidly rose and fell (clusters II and III) were generally more highly induced partly because the baseline transcript levels were relatively low. However, this is not the only explanation as the median basal levels of RNA within each of the transcriptome clusters is relatively comparable, but clusters II, III, and VI are modestly higher than clusters I, IV, and V (**Fig 3D**). The other reason high induction magnitudes are observed for most genes in cluster II and III is due to the high absolute transcript levels one hour after stimulation. For most genes in these clusters, high transcript levels result from robust transcription and not RNA stability, as their half-lives are relatively short (discussed in more detail in following sections).

We also looked to TLR4 stimulation via LPS treatment as a means of comparison with BCR stimulation and found that total genome-wide RNA induction was less robust than with BCR stimulation. It was previously reported that most differentially expressed genes were shared between LPS and BCR activation, but this did not take either the kinetics or magnitude of expression into account [65]. More genes were induced between 10- and 100-fold in response to BCR crosslinking than with TLR stimulation at every time point we assayed (**Fig 4A**). Finally, the transcriptome of B cells in response to stimulation through the BCR is unique as TLR stimulation neither induces the same genes nor does it display the same kinetics as BCR-induced gene expression, especially in the case of “immune cluster genes” (**Fig 4B**). BCR crosslinking, therefore, induces a unique stimulus-specific transcriptional program that reflects the biology of B cells that are stimulated through the antigen receptor.

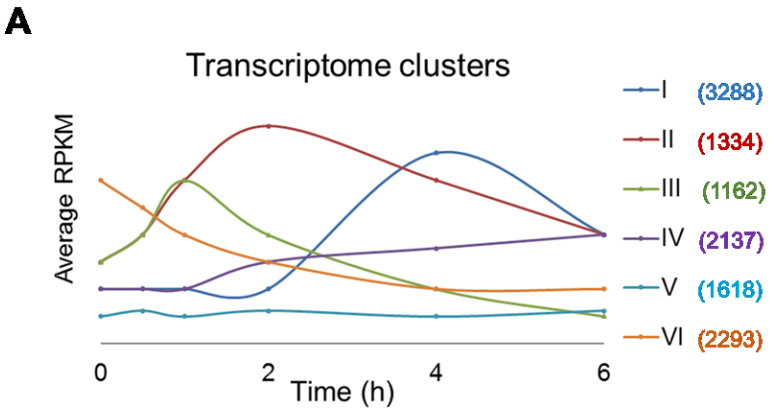

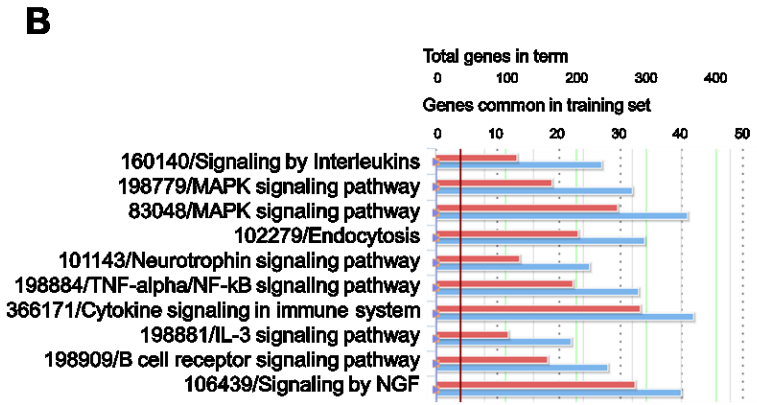

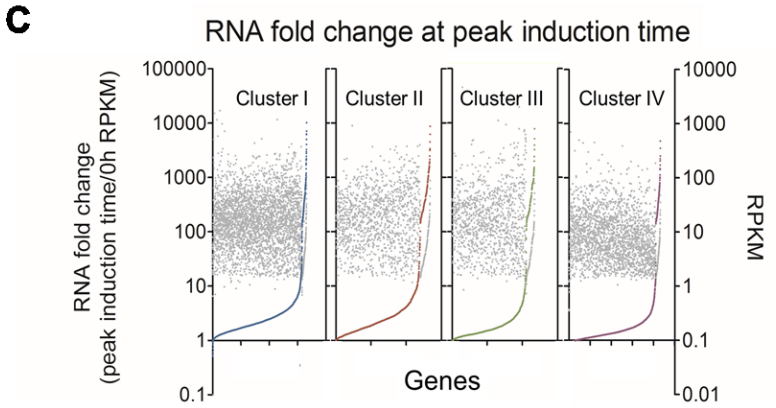

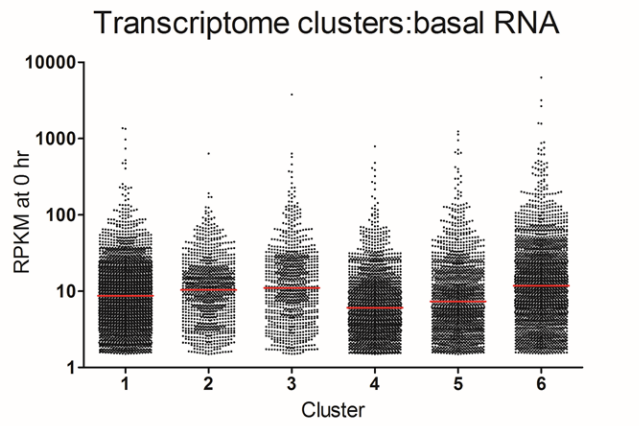

f transcriptional response to B

Figure 3. **Kinetics of transcriptional response to BCR stimulation**

A) Representative kinetic profiles of transcripts based on k-means clustering derived from RNA-seq values across a 6-hour time course.
B) Gene ontology enrichment analysis of cluster III genes. “Total genes in term” refers to number of genes within the indicated pathway according to BioSystems: REACTOME and “genes common with training set” refers to number of genes shared between the input gene list and the designated genes within a pathway.
C) Fold change of RPKM at peak RNA induction time within each transcriptome cluster.
D) Basal (0 h) RPKM values of genes for each of the six transcriptome clusters.

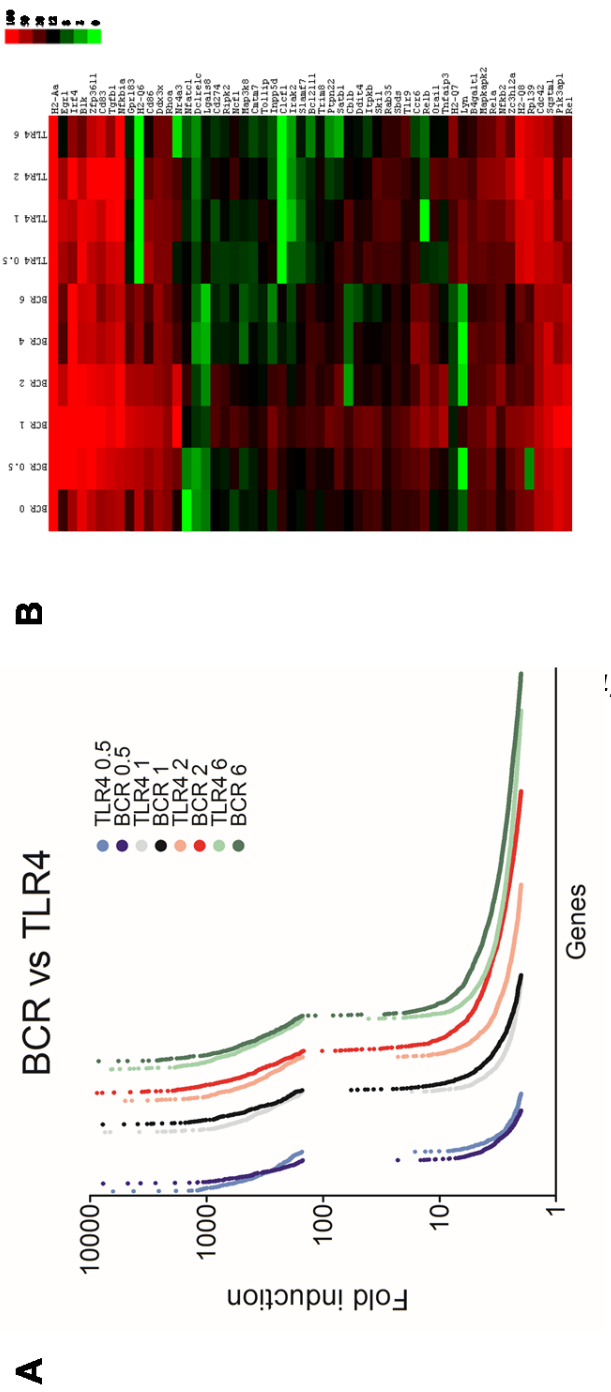

. Comparison between TLR4 and BCR s

Figure 4. Comparison between TLR4 and BCR stimulation

A) Fold induction of RNA (≥2) at 0.5, 1, 2, and 6 hours compared to 0 h in B cells stimulated via BCR (anti-IgM) and TLR4 (LPS).

B) Heatmap of “immune cluster genes” from transcriptome cluster III for both BCR and TLR4 activated time courses.

Genome-wide inducible RelA binding in anti-IgM stimulated B cells.

To elucidate the role of RelA in BCR-induced gene expression, we performed RelA ChIP-seq and looked to genes that demonstrate BCR-specific inducible RelA (iRelA) binding one hour after stimulation. We set the following criteria to stringently identify inducible binding of RelA genome-wide in response to BCR signaling. We restricted our analyses to genes that are reproducibly represented across two biological replicates, set a minimum peak intensity cutoff of 10, and used a cutoff of ≥2-fold enrichment of RelA binding between zero and one hour. For analysis purposes, we partitioned the genome into three regions: promoter, which was arbitrarily defined as -3 kb to +1 kb relative to the TSS, gene body (GB), defined as +1 kb to the termination site, and intergenic, defined as non-promoter and non-GB regions (**Fig 5**). With these criteria, we found a total of 2,026 genes with inducible promoter binding, 1,297 genes with inducible gene body binding, and 729 genes with inducible intergenic region binding (**Fig 6A**). Within each transcriptome cluster, we questioned if iRelA binding occurred selectively in one versus the other and whether this could have any biological implications. Clusters II, III, and VI showed the largest percentages of genes that demonstrated iRelA binding (**Fig 6B**). The transcriptome kinetics of clusters II and III are very similar to the kinetics of nuclear RelA levels in anti-IgM stimulated B cells [76], which led us to further investigate potential RelA dependency of these genes. To determine if there are any patterns in the genomic location of inducible binding and the gene expression kinetics, iRelA patterns were grouped based on binding to various genomic locations (**Fig 6B**). Interestingly, the greatest percentage of iRelA occurred in the promoter regions of genes in all transcriptome clusters, which is contrary to what has been reported

previously [22], but this may be attributable to the variations in categorization of genomic locations and the stringent parameters that we have set for what constitutes inducible transcription factor binding.

To determine if inducibility of RelA binding varies with genomic location (i.e. whether RelA enrichment occurs selectively at different regions of the genome), we compared the fold change of RelA enrichment at one hour after stimulation versus the naive state in each of the three genomic regions (**Fig 6C**). There were two distinct levels of inducible binding; the first level was between 2- and 10- fold and the second was between 10- and 100-fold. As expected, these two levels arise largely as a result of the levels of RelA at baseline, with those that show very high levels of inducibility having very little or no detectable RelA binding at baseline. The highest median level of inducibility occurred at promoters of genes compared to the gene body and intergenic regions, which suggests that iRelA binding at promoters is a *de novo* and directed process. iRelA binding at genic bodies and/or intergenic regions was less robust, which was largely due to prebound RelA instead of low absolute levels of RelA binding at one hour. These results suggest that in response to BCR stimulation, iRelA binding is largely targeted specifically to promoters, which can, in collaboration with other factors, lead to the initiation of transcription.

To relate iRelA binding to a functional output, we looked to the fold changes of RNA at one hour in response to anti-IgM stimulation. Regardless of the genomic region to which RelA inducibly binds, the median fold change in RNA was unchanged (**Fig 6D**). The fact that more than half the genes with iRelA binding do not show a concordant increase in RNA is consistent with previous studies [22], but still surprising, as our analyses applied

more stringent measures in defining RelA binding. One possibility as to why most iRelA binding did not result in a corresponding increase in RNA is due to interplay with other transcription factors that may act as negative regulators of gene expression. Another possibility is the absence of necessary coactivators that are needed to activate transcription. Yet another possibility is that a subset of genes that are RelA dependent bind the TF in a manner that does not fit into the parameters of our analyses (e.g. distal enhancers, promoters outside of the arbitrarily defined region, etc). A better understanding of the factors involved in productive transcription, which we deem as ≥50% increase in basal RPKM, can further our knowledge of RNA regulation. The data also indicates that much of the induced RNA is independent of iRelA binding (**Fig 6D**, last column), which is unsurprising as many other transcription factors, such as NF-AT, are known to be activated in primary B cells [81, 82].

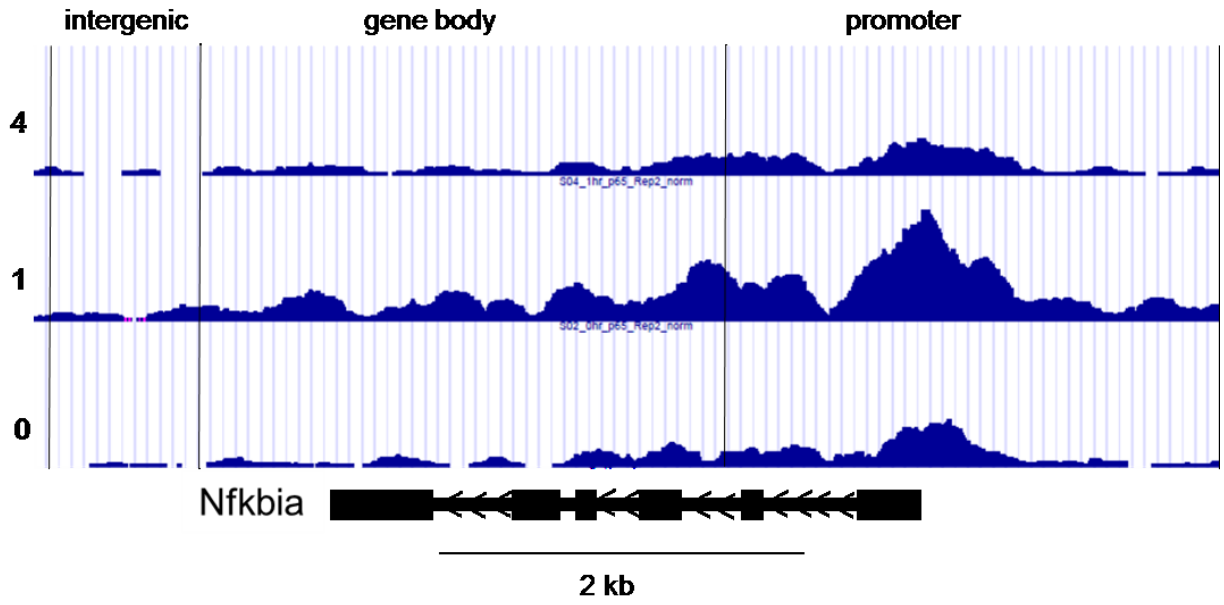

Figure 5. Classification of genomic regions for RelA ChIP-seq analyses.

Figure 5. **Classification of genomic regions for RelA ChIP-seq analysis**

RelA ChIP-seq data was partitioned into three discrete categories for analysis purposes. The promoter was arbitrarily defined as -3 kb to +1 kb relative to the TSS, the gene body (GB) was defined as +1 kb to the termination site, and the intergenic regions were defined as non-promoter and non-GB regions. Peaks within intergenic regions were associated with the genes in the closest proximity.

RelA binding in an

Figure 6. Genome-wide inducible RelA binding in anti-IgM stimulated B cells.

A) Overlap between genes that show inducible RelA binding in either the promoter, gene body (GB), and/or intergenic regions.

B) Breakdown of iRelA binding based on genomic locations within transcriptome clusters. Size of the circles reflects the number of genes within each cluster.

C) Levels of inducibility in RelA binding in promoter, gene body, or intergenic regions.

D) Fold change in RNA as a function of iRelA binding in the designated genomic locations.

Inducible RelA binding relative to pre-existing DNase hypersensitive sites.

We next sought to determine the genome wide status of chromatin accessibility and which sites with iRelA binding were accessible in the naïve state versus those that required chromatin remodeling after stimulation. Several methods, including MNase-seq, DNase I hypersensitivity sequencing, FAIRE-seq, and more recently, ATAC-seq, can be used to determine accessible chromatin regions and mark regulatory regions such as promoters, enhancers, and silencers [83-85]. Thus, we annotated the RelA ChIP-seq peaks with DHS-seq data from primary murine splenic naïve CD43- B cells available from ENCODE. Greater than 90% of inducible RelA peaks in the promoter regions had a preexisting DHS site, while in the cases of both gene body and intergenic regions, roughly 70% of inducible RelA peaks occurred in preexisting DHS sites (**Fig 7A**). These findings are consistent with previously published results across different cell types and stimuli, which have shown that most RelA (and GR) peaks coincide with pre-existing DHS sites [35]. The fact that the percentage of pre-existing DHS sites in the promoter regions of genes with iRelA binding is greater than in the gene body and intergenic regions suggests that pre-existing promoter DHS sites are more susceptible to RelA binding, possibly because of stronger consensus NF-κB motifs and/or other factors that recruit it.

Within each genomic region, we also looked to the percentage of genes with induced RNA expression (**Fig 7A**) and found that approximately 20% of all genes with iRelA binding also have DHS sites and induced RNA. Of the genes that displayed iRelA binding, but no DHS sites, <5% demonstrated inducible RNA across all genomic locations. Further, genes that contain pre-existing DHS sites, have iRelA binding, and

lead to productive transcription appear to be mostly dependent on RelA binding in non-overlapping genomic locations, i.e. the majority of RelA binding occurs exclusively in the promoter, gene body, or intergenic regions (**Fig 7B**). Finally, we looked to the absolute RNA levels of genes with pre-existing DHS sites, iRelA binding at one hour, and at least 1.5-fold induced RNA (**Fig 7C**). RPKM values covered a broad range in all categories, which may be reflective of differential requirements for functional activity of genes and/or multiple mechanisms at work to accumulate or downregulate transcript levels. These results reveal that the pre-existing chromatin structure plays a dominant role in the binding patterns of RelA and, very likely, other TFs. However, there are clearly several layers of regulation post-TF binding that control gene expression, as the final transcript levels of genes with both DHS sites and iRelA binding vary greatly in RNA abundance.

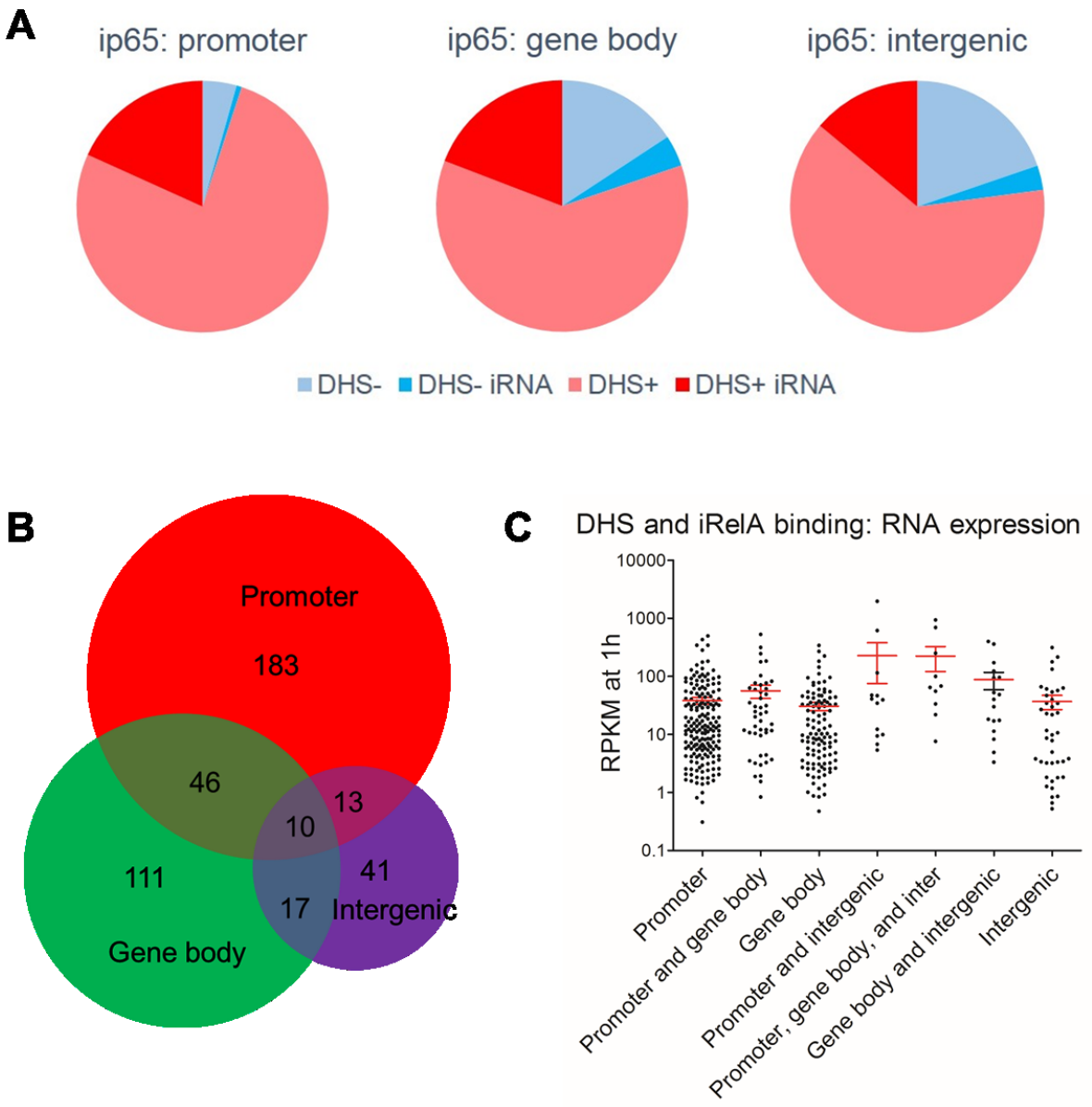

Figure 7. Inducible RelA binding relative to pre-existing DNase hypersensitive sites.

Figure 7. Inducible RelA binding relative to pre-existing DNase hypersensitive sites.

A. Inducible RelA peaks in promoter (L), gene body (M), and intergenic (R) annotated with DNase hypersensitive peaks at 0 h (ENCODE) and displayed as DHS- (no coinciding DHS peak), DHS- iRNA (no DHS, but inducibly upregulated RNA at 1h), DHS+ (coinciding DHS peak), and DHS+ iRNA (DHS and inducibly upregulated RNA at 1 h).
B. Overlap of genes that display iRelA binding within various genomic locations, overlapping pre-existing DHS sites, and inducibly upregulated RNA at one hour.
C. RPKM values of genes at one hour separated based on genomic location of iRelA binding.

Basal state epigenetic and transcriptional status of genes with iRelA binding

Various histone marks and modifications serve as a means by which the status (active vs repressed) of a gene can be determined. H3K4me3, for example, is indicative of active promoters and is often enriched near the TSS of genes [86]. As mentioned previously, the pre-existing epigenetic landscape can lend great insight into RelA binding activity, and consequently, the BCR-induced B cell response. Therefore, we used all available ENCODE and GEO data from primary murine splenic naïve B cells and annotated the status of basal DHS, RNA Polymerase II, H3K4me3, H3K36me3, and H3K27me3 to iRelA peaks. Further, we extended the analysis to include RNA that is induced ≥1.5-fold at one hour after BCR stimulation (productive). From a transcriptional standpoint, we found that approximately 70% of genes with iRelA binding in the promoter contain both a DHS and PolII at the basal level, a small subset of which leads to productive transcription (**Fig 8A**). When we extend the analysis to include genes with H3K4me3 marks, which is associated with transcriptional start sites of actively transcribed genes [86], approximately 50% have H3K4me3 and PolII at the basal level, of which a small subset demonstrate productive transcription (**Fig 8B**). Promoter enrichment analyses using HOMER of these genes that either lead to non-productive or productive transcription revealed that the most enriched motifs were consensus sites for Usf2 and NF-κB/p65, respectively (**Fig 9**). Interestingly, a previous study reported that USF1 and USF2 were enriched in sites that bound NF-κB, especially c-Rel, but lacked consensus NF-κB sites [87]. Thus, it may be possible that p65/c-Rel dimers bind to the non-productive sites, which may be less effective at initiating transcription, despite the presence of TADs in both monomers.

Finally, we looked to H3K36me3, which is deposited in the core and at the 3′ end of active genes, and H3K27me3, which acts as a strong repressive marker [88, 89]. Unsurprisingly, these marks are not highly enriched at the promoters of genes while H3K4me3, a mark largely exclusive to promoters, is highly enriched (**Fig 8C**). Taken together, the data suggests that most iRelA dependent productive transcription occurs in promoters that contain a pre-existing DHS site, H3K4me3, and poised PolII.

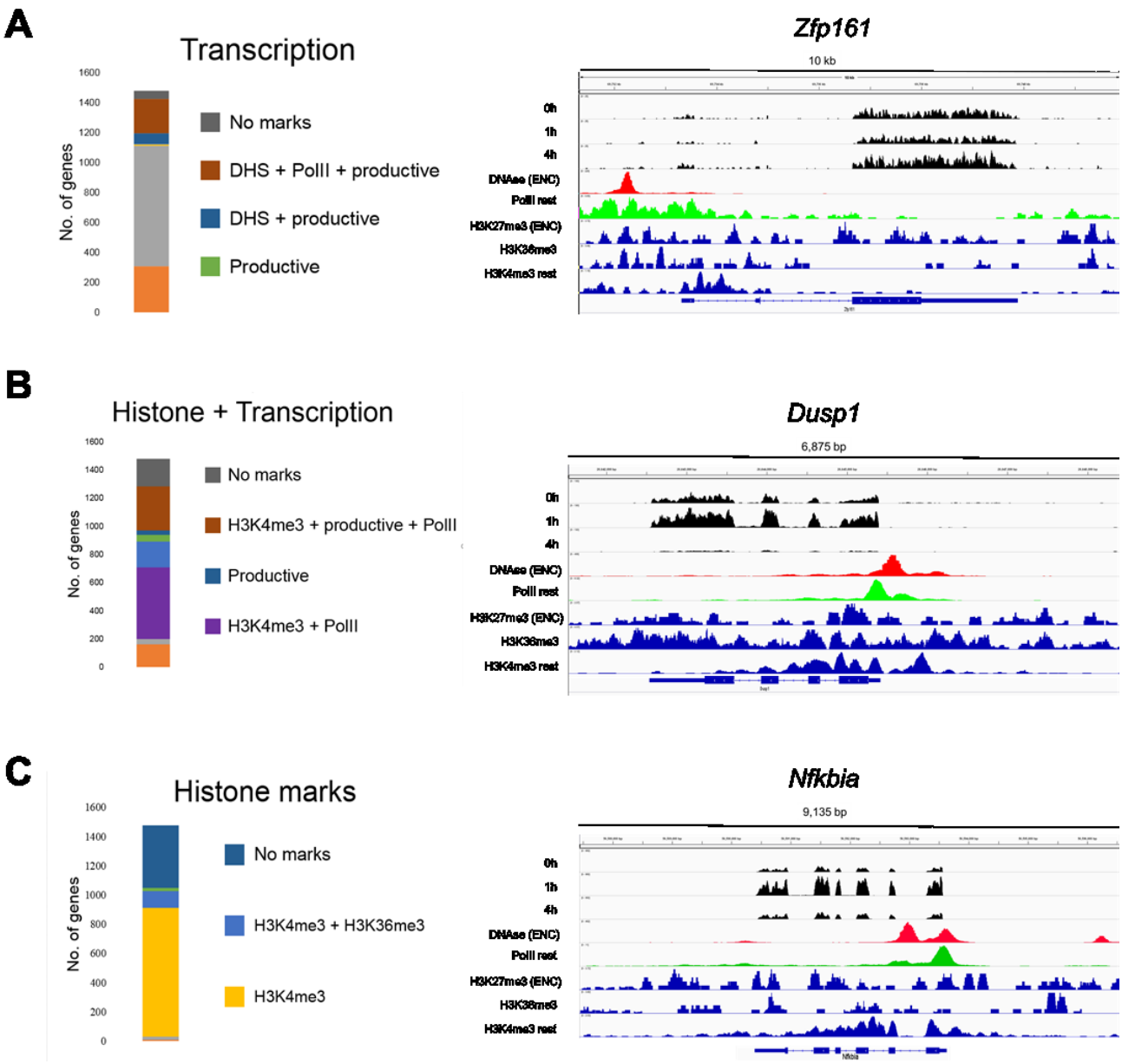

Figure 8. Epigenetic and transcriptional status of resting B cells

Figure 8. Epigenetic and transcriptional status of resting B cells

A. DHS-seq data from ENCODE on CD43- B cells and RNA PolIII ChIP-seq data from GEO was annotated to the RelA ChIP-seq dataset and iRelA peaks were scored as overlapping with these features if the distance between peaks was ≤100 bp. Based on RNA-seq data, transcripts that were induced ≥1.5 fold at any time point after stimulation were deemed “productive” and overlapped with the transcription features. Representative IGV tracks from the largest category shown on the right.
B. Same as (A), but does not include DHS sites and instead incorporates H3K4me3 data from GEO.
C. Histone marks H3K27me3 and H3K36me3 from ENCODE were annotated as described in (A) and overlapped with H3K4me3.

A

Rank	Motif	Name	p-value	Log p-value	q-value
1		Usf2 (bHLH)/C2C12-Usf2-ChIP-seq (GSE36030)/Homer	1e-4	-1.140e+01	0.0038
2		NF-kB-p65 (RHD)/GM12787-p65-ChIP-seq (GSE19485)/Homer	1e-4	-1.039e+01	0.0049
3		HOXA2 (Homeobox)/mES-Hoxa2-ChIP-seq (Donaldson_et_al)/Homer	1e-3	-9.116e+00	0.0117
4		Bapx1 (Homeobox)/VertebralCol-Bapx1-ChIP-seq (GSE36672)/Homer	1e-3	-7.625e+00	0.0369
5		NF-kB-p50, p52 (RHD)/Monocyte-p50-ChIP-Chip (Schreiber_et_al)/Homer	1e-3	-7.227e+00	0.0464

B

Rank	Motif	Name	p-value	Log p-value	q-value
1		NF-kB-p65 (RHD)/GM12787-p65-ChIP-seq (GSE19485)/Homer	1e-4	-1.090e+01	0.0065
2		NF-kB-p65-Rel (RHD)/ThioMac-LPS-Expression (GSE23622)/Homer	1e-3	-8.020e+00	0.0524
3		YY1 (Zf)/Promoter/Homer	1e-3	-7.837e+00	0.0524

Figure 9. Promoter motif enrichment of differentially expressed genes.

Figure 9. Promoter motif enrichment of differentially expressed genes.

HOMER analysis of promoters (-400 bp to +100 bp relative to TSS) of genes with ip65 binding at promoter, H3K4me3 and PolII at basal state, and either

A) no productive transcription at any time point assayed after stimulation or

B) productive transcription at any time point assayed after stimulation.

Stimulus specificity of NF-κB in B cells

To better understand the relationship between iRelA binding (promoter, GB, and/or intergenic) and the stimulus-specific transcriptional program, we looked to genes that display iRelA binding after BCR stimulation and compared RNA expression levels in cells treated with another stimulus. Thus, we compared gene expression patterns in B cells stimulated via the BCR or TLR4 based on iRelA binding in response to BCR activation. Because anti-IgM treatment results in the rapid nuclear translocation of RelA while LPS treatment leads to later and more sustained nuclear RelA, we compared gene expression of BCR stimulated cells at one hour to TLR4 stimulated cells at six hours. Intriguingly, genes that inducibly bound RelA and induced RNA after anti-IgM stimulation were largely unique to BCR vs TLR4 stimulation at both one and six hours (**Fig 10A**). Most, but not all, genes induced after BCR stimulation are not induced in response to TLR4 stimulation at either one or six hours post LPS treatment. In accordance with this, genes that show BCR-induced RelA binding and induce RNA after LPS treatment are uniquely upregulated when compared to BCR activation (**Fig 10B**). Genes with iRelA binding and inducibly upregulated RNA after BCR stimulation were enriched for “immune system processes” and “chemotaxis”, whereas genes that are inducibly upregulated after LPS stimulation were enriched for “gene silencing”. This, however, may be due to selecting genes with iRelA binding in response to BCR stimulation instead of LPS stimulation. Taken together, these data strongly suggest that transcriptional control in primary B cells is dependent on iRelA binding and likely dependent on stimulus-specific co-activators and/or repressors.

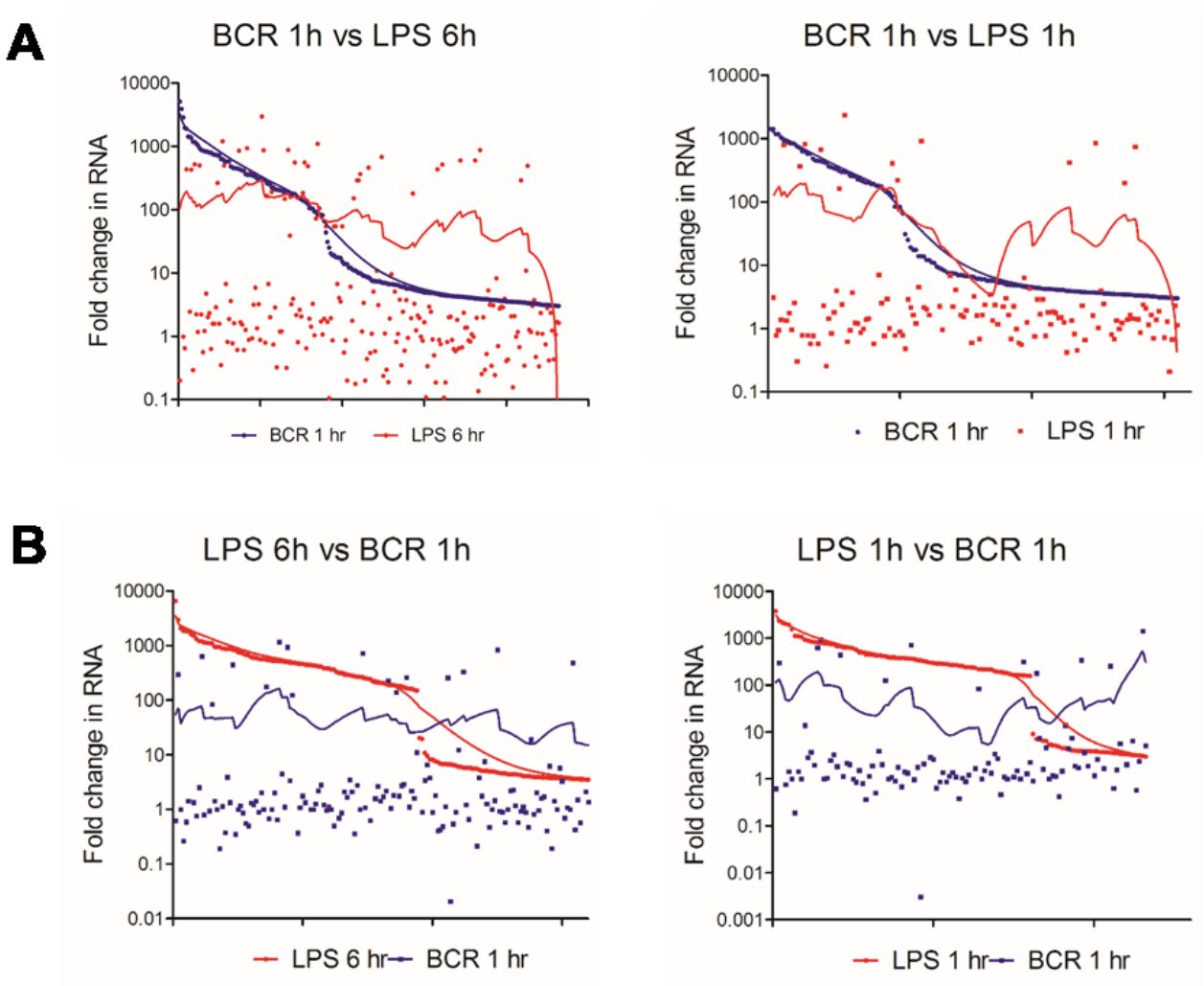

Figure 10. Stimulus-specificity of RelA in B cells

Figure 10. Stimulus-specificity of RelA in B cells

A) Genes that demonstrate iRelA binding (promoter, GB, and/or intergenic) 1h after BCR stimulation and inducibly upregulated RNA by at least 3-fold compared to the level of RNA induction in response to TLR4 stimulation at 6h (L) or 1h (R). Red dots indicate individual fold change of transcript in response to TLR4 stimulation while blue dots indicate BCR stimulation. Solid lines reflect the LOWESS fitted curve for each condition.

B) Genes that demonstrate iRelA binding (promoter, GB, and/or intergenic) 1h after BCR stimulation and inducibly upregulated RNA by at least 3-fold 6h (L) or 1h (R) after TLR stimulation compared to the level of RNA induction in response to BCR stimulation. Red dots indicate individual fold change of transcript in response to TLR4 stimulation while blue indicates BCR stimulation. Solid lines reflect the LOWESS fitted curve for each condition.

Determination of bona fide RelA target genes by use of pharmacological inhibition of IKK-2 and genetic ablation of RelA.

The status of transcription factor binding is often not sufficient for the activation of a gene, which led us to more rigorously define *bona fide* RelA target genes by pharmacological inhibition of IKK-2. We used two IKK-2 inhibitors, BAY 11-7082 and TPCA-1 [90, 91], which ultimately inhibits the nuclear translocation of RelA. B cells were pretreated with IKK-2 inhibitors for one hour prior to activation via anti-IgM. After confirmation that nuclear RelA levels were inhibited after stimulation (**Fig 11A**), we performed RNA-seq on samples treated with inhibitors and anti-IgM to accurately determine genes that were dependent on IKK-2, and by inference, RelA. To validate functional IKK-2 inhibition, we performed qPCR on several putative NF-kB targets (**Fig 12**). Approximately 900 genes were induced ≥1.5-fold with anti-IgM alone at one hour, of which 322 were reduced 75% with IKK-2 inhibition prior to anti-IgM treatment. Of these 322 genes, roughly 40% also displayed iRelA binding (**Fig 11B**). Interestingly, genes that displayed inducible RelA binding in the promoter region (either alone or in combination with gene body and/or intergenic) were most affected by IKK-2 inhibition (**Fig 11D)**. When compared to putative RelA target genes from two different NF-κB target gene databases, only a small number of genes overlapped these lists (**Fig 11D)**, which may either reflect B cell specific genes that are RelA dependent and therefore, not yet curated, or the IKK-2 inhibitors may affect target genes of other transcription factors that are directly or indirectly linked to IKK-2. GO analysis of the 128 RelA target genes revealed enrichment for NFAT-regulated NFAT dependent transcription, TNF

signaling pathway, NF-kB signaling pathway, TCR, and BCR signaling pathways, in which many widely accepted RelA target genes were represented (**Fig 11E**).

Indeed, many genes that would have been categorized as RelA targets based on inducible RelA binding alone were significantly downregulated after treatment with inhibitors. However, there was a larger subset of genes that were downregulated in response to treatment with inhibitors, but did not rely on inducible RelA binding (**Fig 11B**). These 194 genes may be regulated by distal enhancers, which are not accounted for in our definition of iRelA binding. In line with this, it has been previously shown that RelA, in collaboration with other TFs, establishes *de novo* enhancers in macrophages stimulated with lipid A [33]. Collectively, we refer to "RelA target genes" as those that both a) demonstrate inducible RelA binding and b) RNA expression is abrogated by treatment with IKK-2 inhibitors (**Table 1**).

Finally, we used genetic ablation of RelA to strengthen the validity of the genes we have identified as RelA targets based on binding and pharmacological IKK-2 inhibition. Using $RelA^{fl/fl}$ B cells, we treated the cells *ex vivo* with Tat-Cre for 48 hours, which excises the genomic regions between exons 5 to 8 of RelA, leading to non-functional protein (**Fig 13A-C**). qPCR of several NF-kB target genes using *ex vivo* generated $RelA^{-/-}$ B cells revealed were consistent with our binding and pharmacological studies, although genome-wide sequencing has not yet been done (**Fig 14**). Taken together, we have effectively used iRelA binding, pharmacological inhibition of IKK-2, and genetic ablation of RelA to accurately identify and report RelA target genes in BCR-induced B cells.

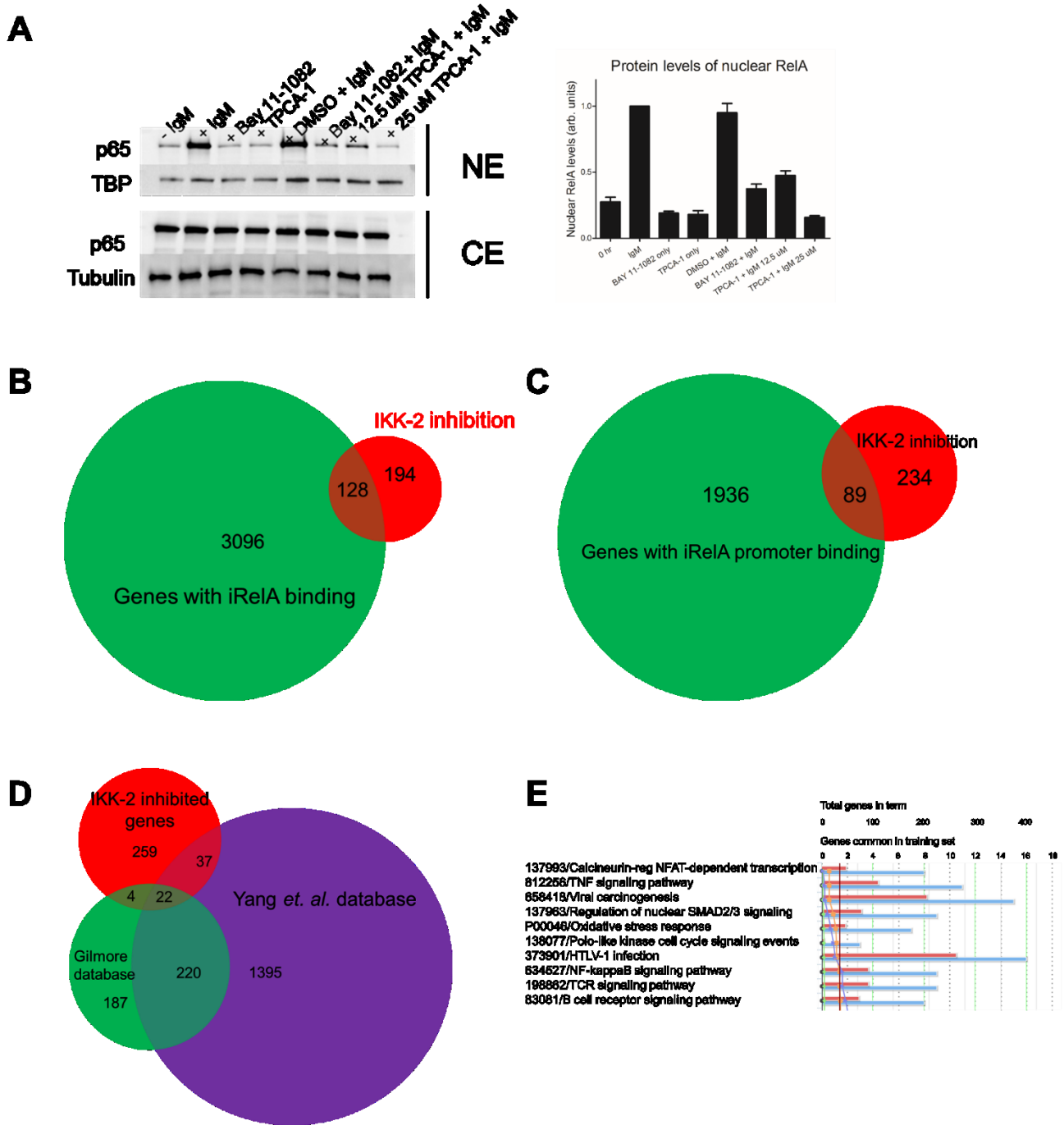

Figure 11. Determination of bona fide RelA target genes by IKK-2 pharmacological inhibition.

Figure 11. Determination of *bona fide* RelA target genes by use of IKK-2 pharmacological inhibition.

A) Nuclear and cytoplasmic levels of RelA in B cells with and without the treatment of two IKK-2 inhibitors, BAY 11-7082 and TPCA-1, followed by anti-IgM stimulation. Western blot quantitation shown on the right.

B) Overlap of genes that demonstrate iRelA binding at any genomic location and inducible genes that are downregulated in the presence of both IKK-2 inhibitors.

C) Overlap of genes that demonstrate iRelA binding in promoters and inducible genes that are downregulated in the presence of both IKK-2 inhibitors.

D) Overlap between genes ≥75% downregulated in the presence of both IKK-2 inhibitors and putative target genes curated by T. Gilmore and Y. Yang.

E) GO enrichment for RelA target genes.

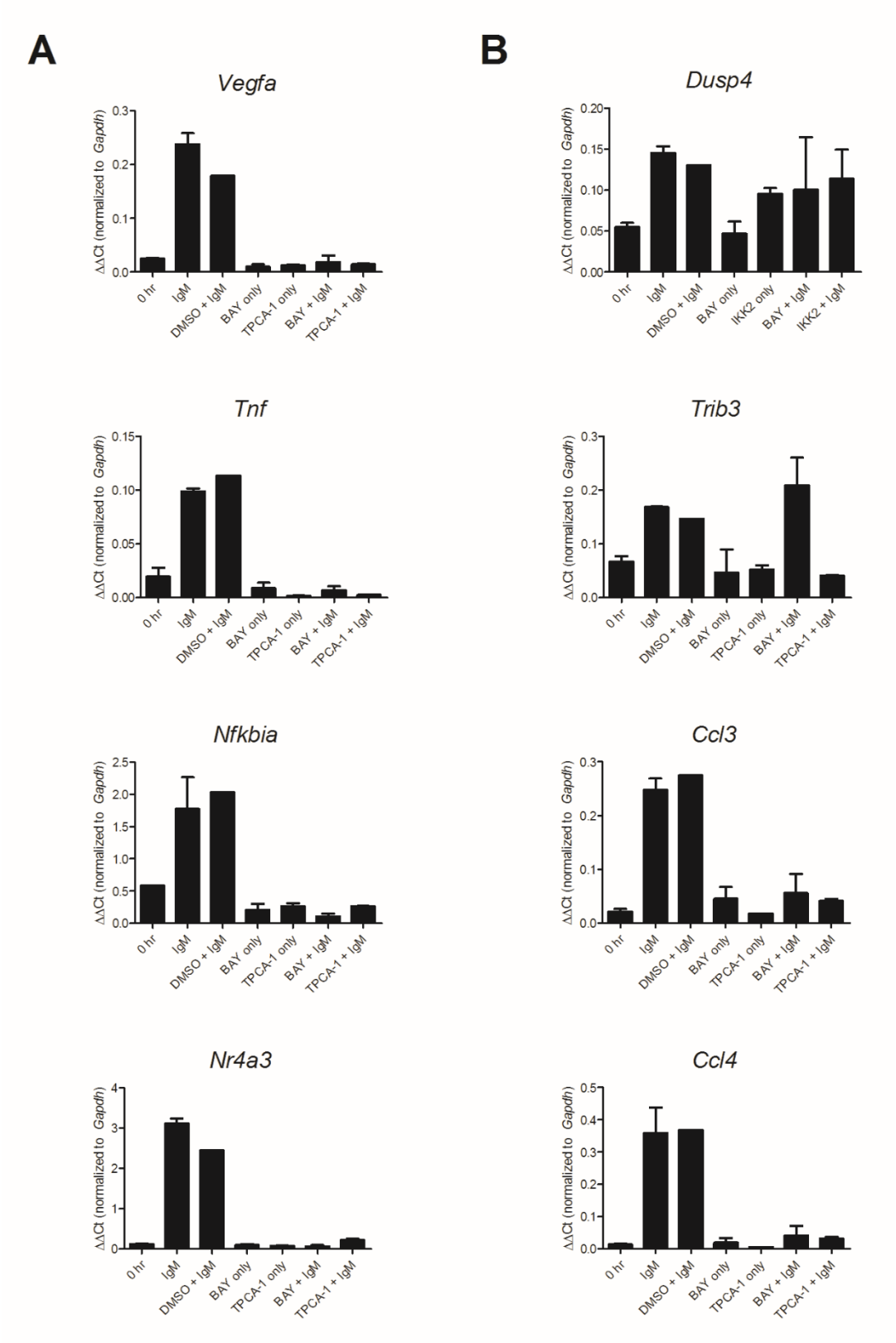

Figure 12. Validation of IKK-2 inhibition

Figure 12. Validation of IKK-2 inhibition

A) Representative profiles of RNA levels measured by qPCR of RelA target genes (iRelA binding and affected by inhibitor) in the presence and absence of IKK-2 inhibition.

B) Representative profiles of RNA levels measured by qPCR of genes with iRelA binding (top two graphs) and without iRelA (bottom two graphs) in the presence and absence of IKK-2 inhibition.

***Table 1**. Genes ≤ 75% inhibited with IKK-2 inhibitors and demonstrate iRelA binding.*			
Synj1	Tgif2	Maff	Nfkbia
Opa1	Elf1	Sqstm1	Ier2
Lrrc32	Pmaip1	Gem	Junb
G3bp2	Fbxo4	Lrmp	Zfp36
Sec24a	Crlf2	Icam1	Nfkbid
Camta2	Nr4a2	Ptpn22	Dusp2
Celf2	Hilpda	Nfkbiz	Srgn
Plk4	Cd274	Ccr7	Rasgef1b
Rhbdd3	Fos	Ptbp1	Cd83
Atl3	Ildr1	Cd72	Med11
Clasrp	E330020D12Rik	Mafk	Litaf
Trim11	Rgs1	Plk3	Gpr183
Bfar	Slc15a3	Snora78	Plek
Ptger4	Crb3	Samsn1	Ccnl1
Eif4g2	Map3k8	Ubl3	Nfkbie
Bbip1	Mir1932	Traf1	Plaur
1600012H06Rik	Timm9	Zc3h12a	Egr2
Arl5b	Slc41a1	Pik3ap1	Ehd1
Eif4a1	Srrd	Tob2	Tgif1
Nub1	Ptp4a2	Stap1	Pim1
P2rx4	Rgs19	Kdm6b	Gadd45b
Rps27a	Txnl4a	Orai1	Myc
Azin1	Grasp	Sub1	Irf4
Alg9	Nampt	Egr3	Rilpl2
Rab20	Slc35b2	Hspa5	Evi2a
2700038G22Rik	Gfi1	Fam43a	Snhg9

Phlda1	D1Ertd622e
Tk1	Dusp1
Dnajb4	Flcn
Ralgds	Prr7
Vegfa	Rel
Dusp10	
Stx11	
Ccdc50	
Dclre1c	
Fen1	
Slc9a8	
S1pr3	
Mreg	
Zbtb10	
Skil	
Fosb	
Fcgr2b	
Lmna	
Plekho2	
Cd180	
Fkbp2	
Il1r2	
Mapk6	
Tnfaip3	
Rnf2	
Rabgef1	
Casp4	

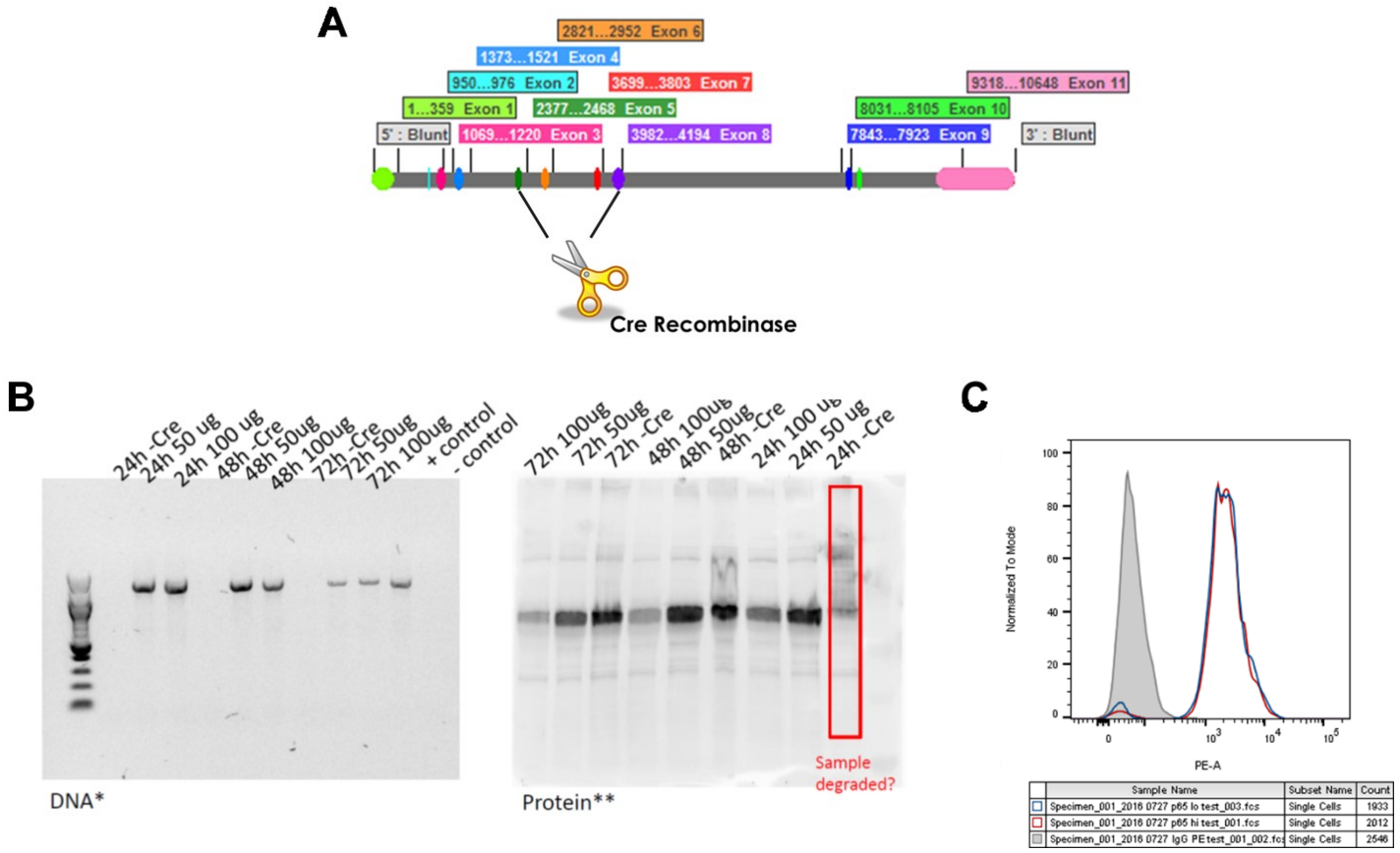

Figure 13. Tat-Cre treatment of RelAfl/fl B cells results in excision of gRelA and leads to decreased protein.

Figure 13. Tat-Cre treatment of RelA$^{fl/fl}$ B cells results in excision of gRelA DNA and leads to decreased protein

A. Schematic of genomic RelA locus with relative positioning of exons; black lines indicate the location of LoxP sites, which are recognized by Cre and lead to the subsequent excision of DNA.
B. Optimization of Tat-Cre treatment using primary RelA$^{fl/fl}$ B cells and varying concentrations of Tat-Cre (50 or 100 ug) and time the cells are harvested after Tat-Cre treatment (24, 48, or 72 hours). (L): DNA samples run on 1% agarose gel and (R): protein samples run on 10% polyacrylamide gel and probed with anti-p65 antibody.
C. RelA$^{fl/fl}$ BB cells treated with 100 ug of Tat-Cre and incubated for 48 hours were fixed and stained with anti-p65 antibody and analyzed by flow cytometry.

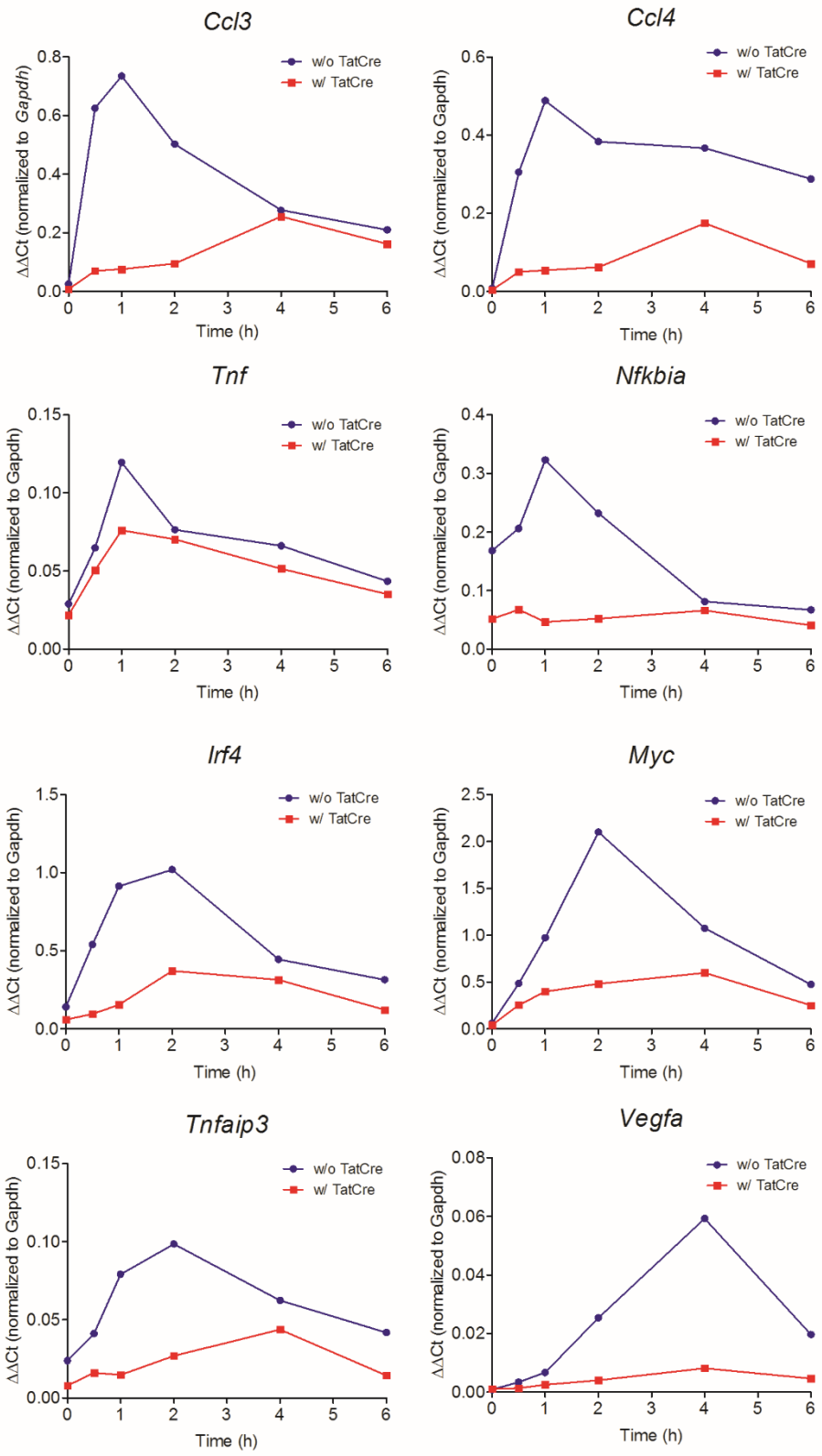

Figure 14. RNA kinetics of select genes after genetic ablation of RelA

Figure 14. Validation of target genes by genetic ablation of RelA using TAT-Cre

Representative qPCR profiles of genes induced within one hour after BCR stimulation in primary B cells treated with Tat-Cre for 48 hours.

Potential RelA dependent distal regulation of CCL3 and CCL4

Despite the stringent conditions we applied in our ChIP-seq analyses, we did not account for genes that are regulated via distal enhancers. Previous reports have indicated that the majority of binding sites of signal-dependent transcription factors are in distal intra- and intergenic locations that exhibit enhancer-associated histone marks [33]. This report indicated about 50% of "enhancer-like" regions were intragenic, which in our analyses, would be defined as gene body. Our analyses found the greatest level of inducible RelA binding in the promoter of genes and the genes that were most affected by IKK-2 inhibition were those that inducibly bound RelA. Of particular interest, however, are the genes that were affected by treatment with IKK-2 inhibitors and yet did not depend on RelA binding. As seen in **Fig 15A**, three genes with fast, exponential decay (addressed in the following chapter), *Plau*, *Ccl3*, and *Ccl4*, in the "no iRelA" category are strongly induced and have been previously curated as putative NF-κB target genes [92], but there was no detectable constitutive or inducible binding of RelA in their promoters or gene bodies. Because initial studies that deemed Ccl3/4 as NF-κB target genes were done in a human cell line system using a luciferase assay under the control of strong RelA binding motifs, it can be argued that the modes of regulation differ between species, but RelA also seems to play an essential role in the regulation of mouse*Ccl3* and *Ccl4.* Pharmacological and genetic perturbation of the canonical NF-κB pathway dramatically decreased production of *Ccl3* and *Ccl4* transcripts, indicating that NF-κB is playing a critical role in their expression patterns (**Fig 15B**).

Approximately 7 kb upstream of the CCL3 gene, there is a stretch of DNA that is DNAse hypersensitive, H3K27ac, and H3K4me3 positive, and is enriched for PolII (**Fig 20C**,

left)**.** There is also a modest inducible p65 peak overlapping this putative regulatory region, although this peak does not score in our analyses due to the stringent parameters (**Fig 20C**, right). Based on the enrichment of these factors, we postulate that RelA is involved in the regulation of CCL3 and CCL4 by this regulatory region, but this warrants further analysis. Nonetheless, this example highlights instances in which RelA-dependent regulation of gene expression are less straightforward than promoter binding leading to transcription.

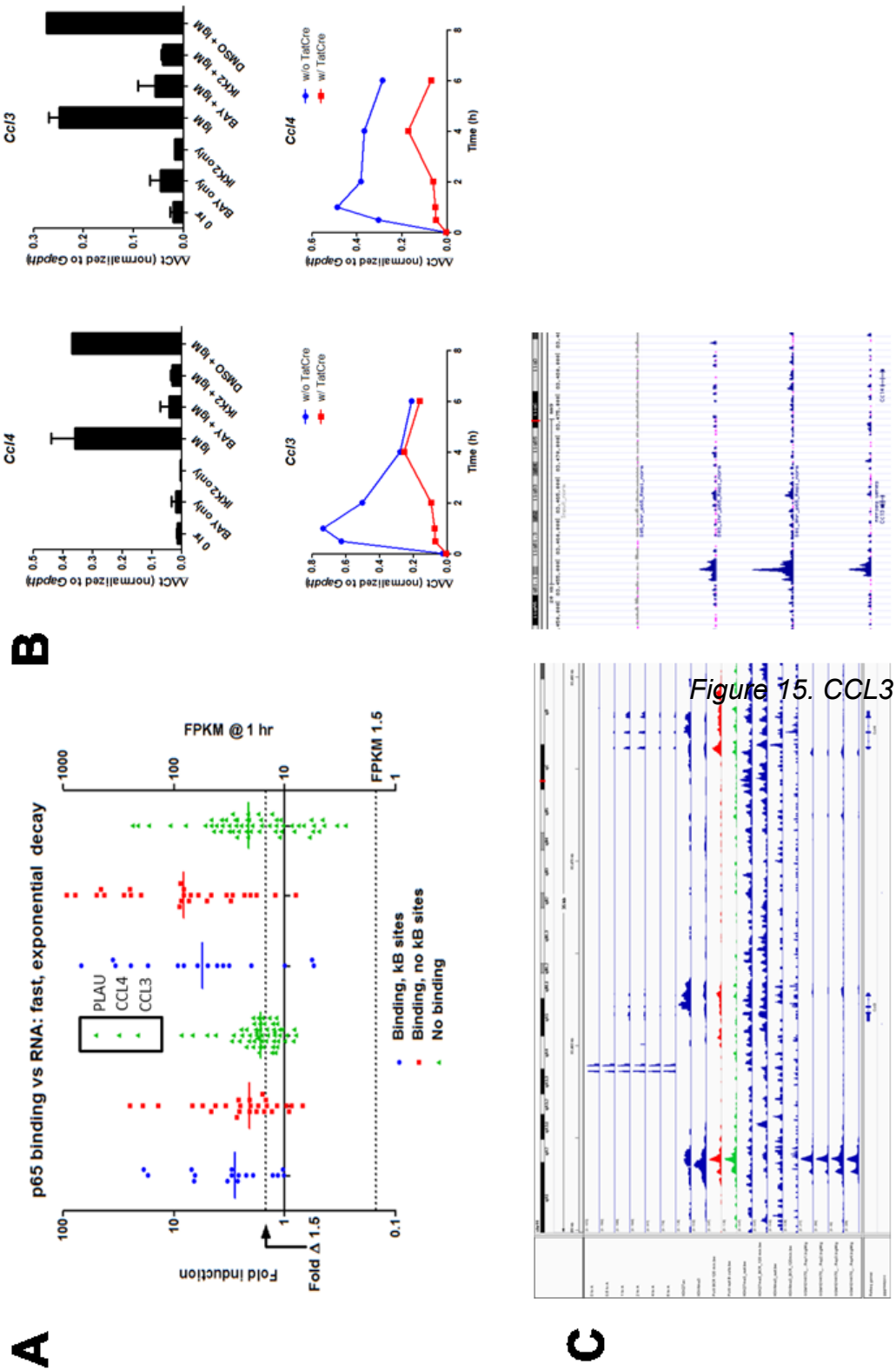

Figure 15. CCL3 and CCL4 regulation b

Figure 15. CCL3 and CCL4 regulation by RelA

A. Genes with fast exponential decay were separated into categories of iRelA binding with κB sites under the peak, iRelA binding with no κB site under the peak, and no iRelA binding and graphed according to RNA fold induction and RPKM.
B. Top: RNA expression levels of *Ccl3* and *Ccl4* in WT B cells treated with IKK-2 inhibitors and bottom: RelAfl/fl B cells treated with Tat-Cre.
C. (L): RNA-seq and histone mark profile of *Ccl3* and *Ccl4* and (R): RelA ChIP-seq profile.

Chapter III: mRNA decay of RelA-dependent genes in BCR-stimulated B cells

Introduction

Steady state gene expression is a comprehensive output of transcription (synthesis) and mRNA decay. The decay of mRNA is arguably as important as its synthesis, especially in the context of proinflammatory cytokines and chemokines [93]. For example, dysregulated TNFα synthesis and/or decay will likely result in a chronically hyperinflammatory milieu *in vivo*, which can lead to serious pathological consequences. Several methods now exist to determine mRNA decay rates, such as treatment with transcription elongation inhibitors, metabolic labeling, and isolation of chromatin, followed by genome-wide sequencing [61, 93, 94]. Many studies (addressed in a following section) have looked to global mRNA decay rates and half-lives using various methods in different cell types in response to diverse stimuli, but very few studies look to primary cells. Therefore, the goal of our study is to determine genome-wide mRNA half-lives in primary BCR-induced B cells, especially in the context of NF-κB-targets, to gain a better understanding of the total life cycle of an NF-κB target gene.

Factors involved in mRNA stability

mRNA stability can be regulated by myriad processes, including RNA-binding protein (RBPs), miRNAs, lncRNAs, etc. The 3' untranslated region (UTR), defined as the region of mRNA between translation termination codon and the polyA-tail, is widely accepted as an important cis-regulatory element that recruits factors, such as RBPs and non-coding RNAs, involved in the regulation of mRNA stability (reviewed in [95]). As shown in **Fig 16A**, AU-rich sequence elements (AREs) are contained within most 3' UTRs and are necessary for the recruitment of specific proteins, such as TTP or HuR, that result in

the either decay or stability of the mRNA, respectively (reviewed in [96, 97]). Apart from AU-rich elements, 3' UTRs often contain other sequence elements that recruit specific RBPs and affect mRNA stability. For example, CUG triplet repeat RNA-binding protein 1 (CUGBP1) binds to embryo deadenylation element (EDEN)-like sequences, leading to the deadenylation and destabilization of mRNA [98]. On the other hand, polypyrimidine tract-binding protein (PTB) binds to UC-rich elements and stabilizes mRNA [99] (**Fig 16B**). Noncoding RNAs, such as miRNAs, play an integral role in the regulation of mRNA stability by binding to specific anti-sense sequences in the 3' UTRs of genes and recruiting the RNA-induced silencing complex (RISC), which ultimately leads to deadenylation and mRNA decay (**Fig 16C**). Finally, nonsense mediated decay (NMD) is an mRNA degradation process that protects against deleterious truncated proteins encoded by mRNA with premature termination codons (**Fig 16D**).

Yet another mechanism to control gene expression is alternative polyadenylation (APA), the addition of a poly(A) tail to a messenger RNA to multiple possible sites within a gene, resulting in either a quantitative or qualitative change in gene expression. In coding-region APA (CR-APA), the alternative poly(A) sites are located within introns or exons, which may result in different protein isoforms. For example, during the B cell transition to a plasma cell, the membrane-bound form of IgM switches to the secreted form due to CR-APA [100-102]. In UTR-APA, the alternative poly(A) sites are located within the 3' UTRs, which results in transcripts with varying lengths of 3' UTRs, potentially leading to transcript differential regulation (reviewed in [103]).

Clearly, there are many possible ways by which mRNA stability is regulated, indicating that it is while many factors can lead to increased or decreased stability, it is also a

tightly controlled mechanism. This rigorous regulation is an important feature in eukaryotic cells as levels of RNA must be appropriately modulated in response to stress or stimuli to elicit the proper outcome.

Mammalian mRNA half-lives

An early study that sought to determine mRNA half-lives on a genome-wide level in mouse embryonic stem cells found the median RNA half-life to be roughly 7 hours. They identified less than 100 genes that had half-lives less than one hour, which were enriched for regulatory functions [104]. In line with this, Friedel *et al* determined half-lives of transcripts in mouse and human B cells and fibroblasts and found that in both species, transcripts with short half-lives were involved in transcription regulation and signal transduction, whereas transcripts with longer half-lives were involved in cellular metabolism. Further, this study compared half-lives determined by either addition of actinomycin D or 4-thiouridine (4-SU) incorporation followed by sequencing. Based on their analyses, they reported that actinomycin D treatment may provide less accurate half-lives for transcripts that have slow decay, but transcripts with fast (less than six hours) decay can be determined with as much accuracy as treating the cells with 4-SU [105].

Raghavan et al determined half-lives of roughly 6,000 RNA transcripts using actinomycin D followed by microarray of primary human T lymphocytes stimulated with anti-CD3 or anti-CD3 and anti-CD28. The largest proportion of transcripts had long half-lives (>6 hours), with a much smaller proportion of transcripts having very short half-lives. When looking exclusively to the subset of transcripts that are induced 5-fold or more upon stimulation (either anti-CD3 and anti-CD28 or anti-CD3 alone), the largest

proportion of transcripts had very short half-lives (<60 min). These short-lived genes were enriched in the biological processes such as cytokines, signal transduction regulators, transcription factors, and regulators of apoptosis. When looking to the AREs in the 3' UTRs of genes in T cells, approximately a quarter of genes had rapid decay, half had intermediate decay, and the remaining had slow decay. Thus, while AREs may be important for a subset of genes with rapid decay, it is clearly not the only element at play in regulating the decay of transcripts nor is it sufficient for the decay of transcripts.

Coordinated regulation of transcription and mRNA decay

Studies in yeast were the first to report evidence of promoter elements dictating RNA stability [106, 107]. Bregman *et al* observed that upon changing the upstream activating sequence (UAS) of promoter elements in yeast, decay kinetics of transcripts are altered [106]. Haimovich et al found that perturbations of mRNA decay machinery led to global dramatic changes in the transcription patterns as well [107]. Since then, the concept of communication between the 5' and 3' ends of genes has gained considerable momentum. A recent study done in HeLa cells found that the transcription factor, Erg, was necessary for the recruitment of the decay machinery, CCR4-NOT, via its interaction with an RBP, RBPMS [108]. However, it was not clear whether the transcripts that were dependent on Erg for their decay were also induced by the same transcription factor. Taken together, accumulating evidence is strongly suggestive of gene expression as a circular process, with transcription factors affecting mRNA stability and stability factors affecting transcription.

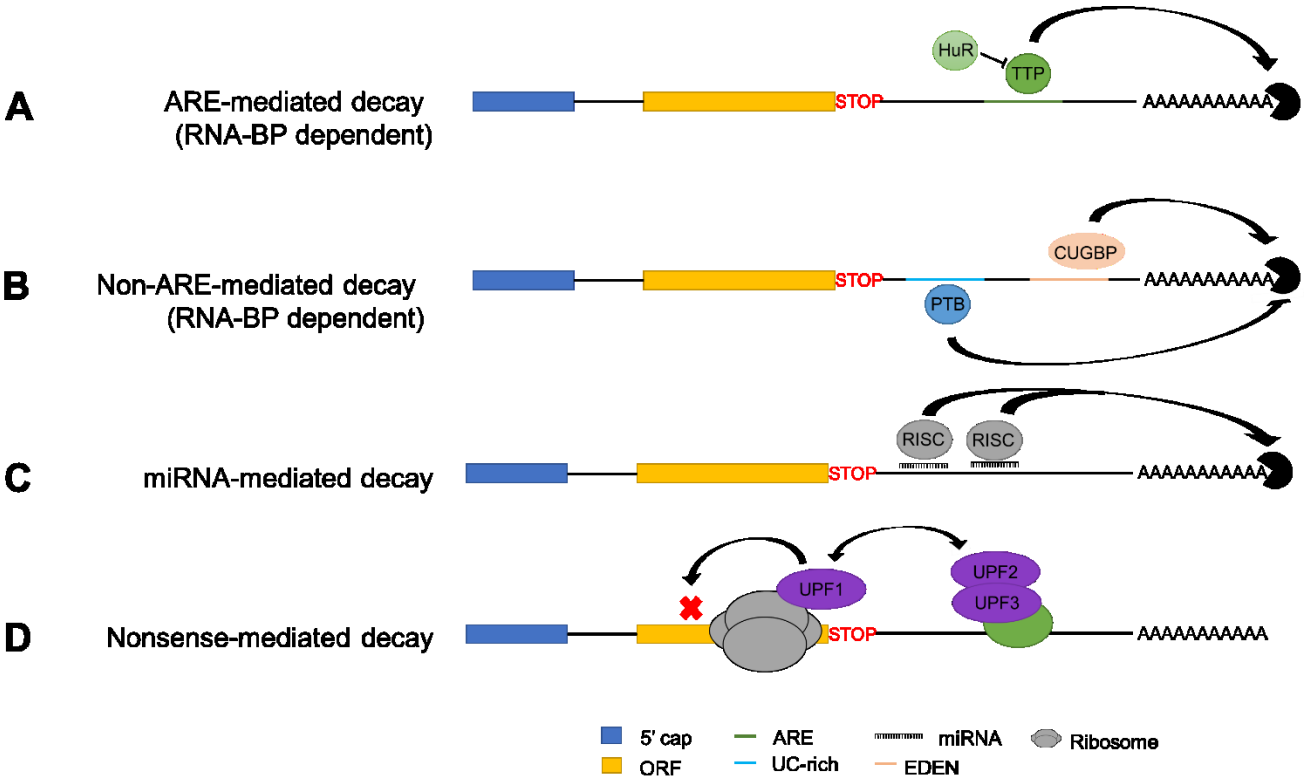

*Adapted from [109]

Figure 16. Modes of mRNA stability

Figure 16. Modes of mRNA stability

A. AU-rich element (ARE)- mediated decay: sequence-encoded AU-rich elements recruit RNA binding proteins (RBPs) such as tristetraprolin (TTP), which subsequently results in mRNA deadenylation and decay. RBPs such as HuR may act to oppose the functions of TTP, resulting in increased mRNA stability.
B. Non-ARE-mediated decay: RBPs, such as CUG triplet repeat RNA-binding protein 1 (CUGBP1), bind to embryo deadenylation element (EDEN)-like sequences, destabilizing mRNA. Conversely, RBPs such as polypyrimidine tract-binding protein (PTB) bind to UC-rich sequences and stabilize mRNA.
C. microRNA-mediated decay: miRNAs (20-24 nt) bind to specific seed sequences in 3' UTRs and recruit RNA-induced silencing complex (RISC), leading to deadenylation and degradation of mRNA.
D. Nonsense-mediated decay: mRNAs harboring premature termination codons are selectively degraded through interactions between regulator of nonsense transcripts (UPF) proteins, leading to cleavage of the transcript.

Decay kinetics of BCR-inducible genes

As mRNA levels are a comprehensive readout of both the transcription and decay of mRNA, we looked to the decay kinetics of RNA to get a complete picture of the levels at which NF-κB-dependent mRNA is regulated. Therefore, we determined the half-lives of > 1,200 genes by blocking transcription using the PolII inhibitor, actinomycin D (ActD), and tracking the decay pattern of the residual RNA. As shown in **Fig 14A**, one hour post stimulation with anti-IgM, cells were treated with ActD and harvested at discrete timepoints across a six hour time course and the RNA was subsequently subjected to microarray. Despite the different platforms used to measure mRNA kinetics for steady-state (RNA-seq) and decay rates (microarray), the two datasets were consistent such that joint analysis is justified (**Fig 15**). To avoid false- positives and artifacts, we applied a series of stringent criteria on the data derived from the microarray. The raw intensity values from the microarray at any timepoint for all probes must exceed 150, induction levels must be at least 1.3-fold, and RNA maxima must occur at either 1 or 2 hours, coinciding with RelA nuclear expression levels, after ActD treatment. For a detailed explanation of how RNA half-lives were determined, see **Materials and Methods**.
We divided the genes based on the decay kinetics of genes as either fast (≤70 min), intermediate (70-240 min), or slow (≥240 min) and further subdivided them as exponential or nonexponential decay. We found 154 genes with t1/2 ≤70 min, 559 with t1/2 between 70 and 240 min, and 507 with t1/2 ≥240 min. The majority of genes with fast decay (128/154) showed exponential decay, while those with slow (437/507), and to a lesser extent, intermediate (358/559), decay showed mostly nonexponential decay (**Fig 14B)**. The majority of genes demonstrated slow, nonexponential decay, which is

consistent with the decay pattern of genes in primary T cells stimulated with CD3/CD28 [110]. To ensure that the microarray-derived half-lives were reliable, we confirmed half-lives of many genes using qPCR, which provided similar results (**Fig 14C**). As has been previously demonstrated in fibroblasts stimulated with anti-TNF, genes with fast, exponential decay show a GO enrichment for cytokine activity [60] (**Fig 14B**). When we compared the induction of RNA to their half-lives, we found that highly induced RNA displayed faster half-lives than those that had lower induction, consistent with previous findings [60] (**Fig 16A**). The transcriptome profiles of genes among each of the decay categories were relatively comparable and mostly enriched for clusters I, II, and III (**Fig 16B**). This is unsurprising as one of the criteria for genes chosen for decay analysis was the induction of RNA at one or two hours after stimulation. Finally, we also looked to the prevalence of inducible RelA binding in genes from each of the decay categories and found that genes with faster decay kinetics show a higher proportion of inducible RelA binding in the promoter, gene body, and/or intergenic regions (**Fig 16C**).

ay kinetics of BCR-inducible

Figure 17. **Decay kinetics of BCR-inducible genes**

A) Top: experimental schema outlining sample treatment and collection; bottom: numbers of probes from microarray after application of various criteria.

B) Profile of B lymphocyte mRNA decay categorized by fast (<70 min), intermediate (70-240 min), and slow (>240 min), exponential, or nonexponential degradation. Genes with fast, exponential decay displayed enrichment for cytokine activity and cytokine receptor binding.

C) Representative profiles of genes (*Nfkbia* and *Ccl3*) with both microarray- and qPCR- derived half-lives.

een microarray an

Figure 18. **Comparison between microarray and RNA-seq datasets**

Fluorescent intensity values from microarray were log2 transformed and plotted against (log2 transformed FPKM + 1) values from RNA-seq dataset. Correlations of all timepoints were determined using the R^2 value.

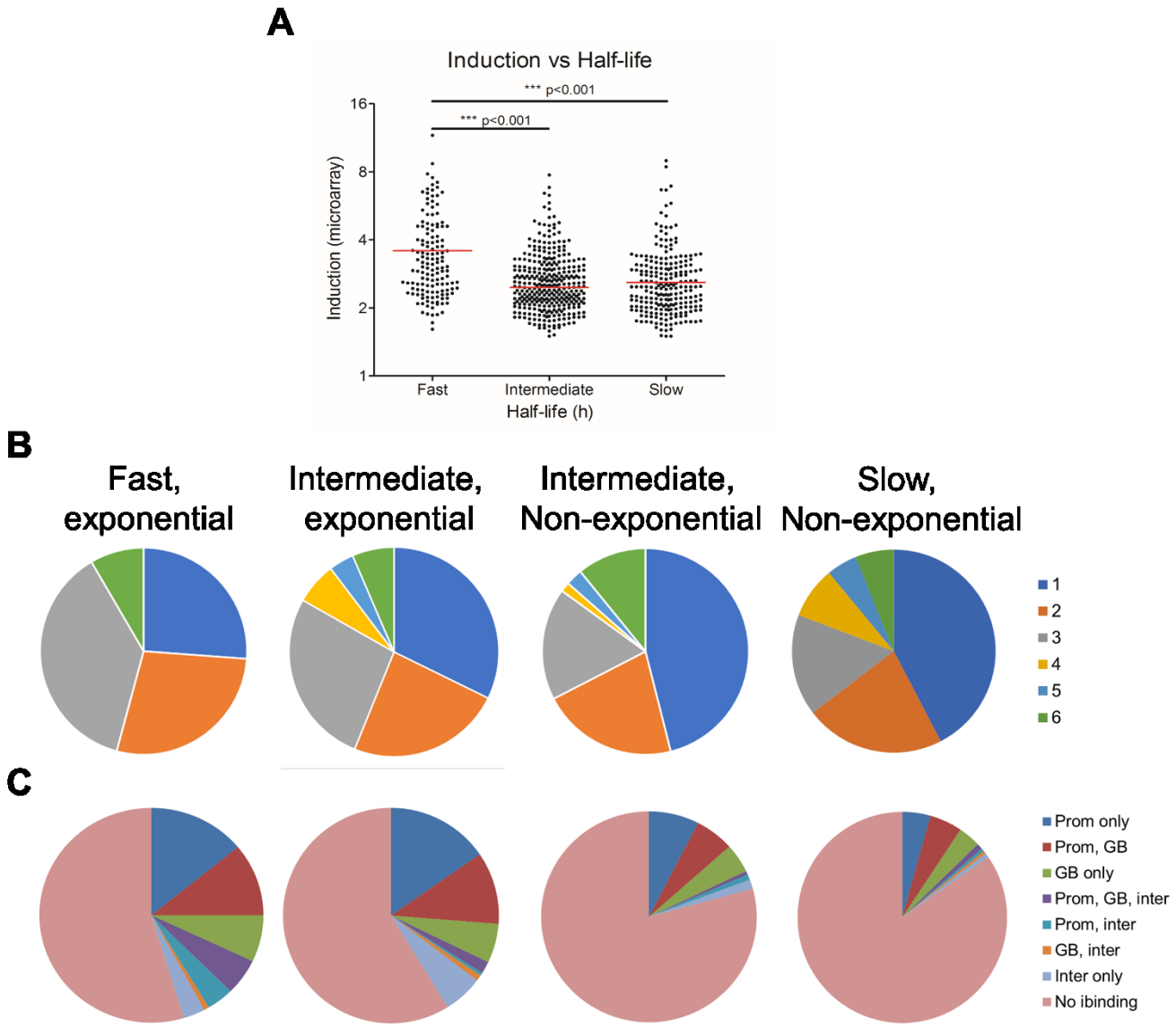

Figure 19. Relationship between ip65 cistrome, transcriptome, and mRNA stability

Figure 19. Relationship between ip65 cistrome, transcriptome, and mRNA stability

A) Induction vs. half-life of RNA based on values derived from microarray. Red lines indicate median fold-change in RNA induction.

B) Division of genes within each decay category into transcriptome clusters (based on **Fig 3A**).

C) Division of genes within each decay category based on iRelA binding.

hnRNPA1, in part, mediates rapid decay of many RelA-dependent genes

The simplest interpretation of exponential vs nonexponential decay is a single- vs multi-step decay mechanism, respectively. Therefore, we looked to the 3' UTRs of fast, exponential decaying genes for common regulatory features that may explain similarities in RNA stability. To determine if alternative polyadenylation can account for differential decay patterns, we used the bioinformatics algorithm "Dynamic analyses of alternative polyadenylation (APA) from RNA-seq" (DaPars) to quantify relative APA usage. DaPars directly infers dynamic APA events through comparison between different conditions. For a given transcript, DaPars first identifies the *de novo* distal polyA site based on a continuous RNA-seq signal independent of the gene model and uses a linear regression model to identify the location of a *de novo* proximal polyA site as an optimal fitting point [111]. As can be seen in **Fig 20A**, there were very few APA events in the 3' UTRs of genes that are induced at 1 hour and although the number increases when looking to the coding regions (CR) of genes, genes that demonstrate fast decay are not represented. Thus, APA events do not play a significant role in the rapid decay of BCR-inducible genes.

As it has been previously proposed that 3' UTR lengths and correlate with RNA stability, we first compared 3' UTR lengths between the three decay categories, but did not find a significant difference (**Fig 20B**). 3' UTRs contain binding motifs for miRNAs and RNA binding proteins (RBPs) and have been reported in several contexts to regulate RNA stability. Consequently, we looked for the enrichment of RBP motifs within the 3' UTRs of genes with fast, exponential decay (**Fig 21A**). One of the top binding motifs, hnRNPA1, was found to be highly expressed in primary B cells at both the RNA and

protein levels (**Fig 21C and D**). hnRNPA1, one of several hnRNP family members, has been strongly linked to mRNA processing, especially in splicing, but has also been recently implicated in RNA stability [112, 113]. Hence, we used siRNA to knock down hnRNPA1 in two mature B cell lines, M12 and Bal17, which resulted in modest reduction of hnRNPA1 protein (**Fig 22A**), but significant reduction in mRNA (**Fig 22B**). We subsequently looked to the stability of several genes outlined in **Fig 22C-E**, which either did or did not demonstrate iRelA binding.

RNA stabilities of genes that demonstrate fast, exponential decay, but do not have hnRNPA1 binding motifs in their 3' UTRs were unaffected by hnRNPA1 knockdown (**Fig 19B**). Several, but not all, genes that inducibly bind RelA and do not induce RNA in the presence of IKK-2 inhibitors (i.e. RelA target genes) result in longer half-lives after hnRNPA1 knockdown (**Fig 19C**). Interestingly, while the half-lives of some non-RelA target genes were also increased after hnRNPA1 KD, a greater number of genes were unaffected. These results suggest that the rapid decay of some transcripts via RNABPs, such as hnRNPA1, is coordinated with its rapid induction via RelA in primary B cells stimulated via the BCR.

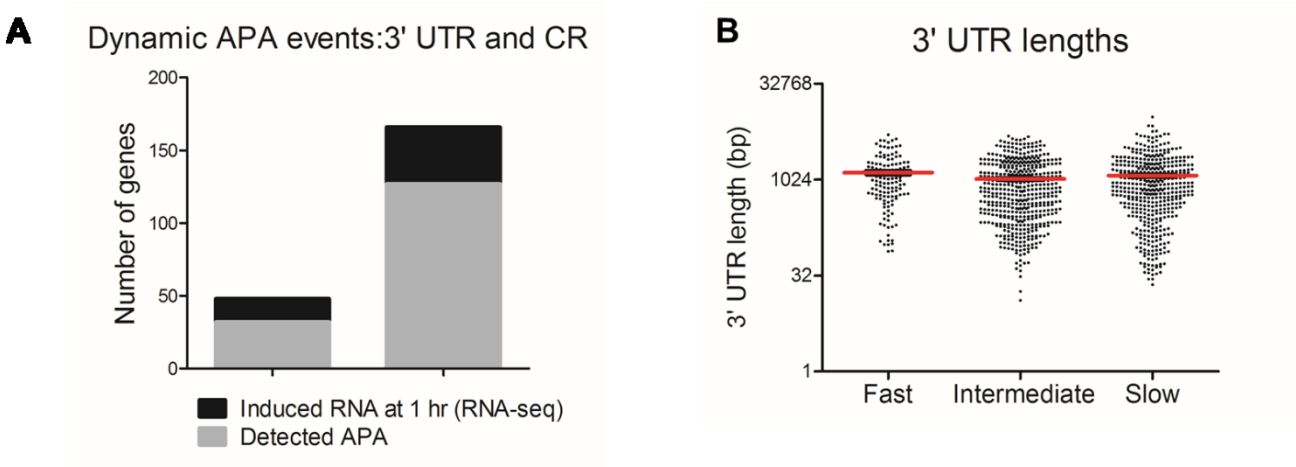

Figure 20. APA events and 3' UTR analyses of genes based on decay categories

Figure 20. APA events and 3’ UTR analyses of genes based on decay categories

A) Incidences of APA events (gray) for 3’ UTRs (L) and coding regions (R) of genes across the six hour time course using DaPars. Genes that are induced at 1 hour are highlighted in black.

B) Lengths of 3’ UTRs of genes (retrieved from 3’ UTR database) within each decay category irrespective of exponential or non-exponential decay.

A

Motif Name	Consensus	log(pvalue)
M035_0.6:Lin28a:Lin28b	MGGAGAA	5
hnRNPA1:hnRNPA1_2	GTAGTAGT	4
M037_0.6:Mbnl1:Mbnl2:Mbnl3	NGCTTGC	4
M045_0.6:Pum1	TGTACAK	4
M098_0.6:Pum1	TGTACAK	4
M291_0.6:Eif4b	GCGGRAC	4
M061_0.6:Samd4:Samd4b	GCTGGMC	3
M086_0.6:Srsf10:Srsf12	AGAGAGG	3
M101_0.6:Pum1	TGTAATT	3
M147_0.6:Cnot4	GACAGAN	3
M240_0.6:Rbm24	GWGTGTGD	3
M261_0.6:Sf3b4	GTGTGA	3
M319_0.6:Gm5145:Snrpa:Snrpb2	ATTGCAC	3
M350_0.6:Zfp36:Zfp36l1:Zfp36l2:Zfp36l3	TTATTTATT	3

B

ip65 binding	No ip65 binding
Irf4	Rbbp6
Fbxo4	Zfp655
Uck2	Scyl3
Chd1	Grwd1
Egr2	Wdr75
Wnk1	Cblb
Extl2	Ccr5
Fbxo46	Zscan21
Csf1	Bcl2l11
Gpd2	Ap1g1
Map3k1	Plagl2
Tagap	Zfx
Gch1	Nsf
Tnf	Nt5dc3
Nab2	Exoc8
Plekhm1	Gmppb
Fbxo30	Tle1
Maff	Adnp
Cd83	Cd3eap
Gad1	Rheb
Plcl2	Kras
Smad2	Acbd3
Chst10	Gtf2e1
	Cdkn1a
	Plau
	Cyp51

C

D

Figure 21. RNABP enrichment in 3' UTRs of fast, exp

Figure 21. RNABP enrichment in 3’ UTRs of fast, exponential decaying genes.

A. Motif enrichment analysis of 3’ UTRs from genes in the fast, exponential decay category.
B. Genes with fast, exponential decay and hnRNPA1 motifs in 3’ UTRs that either inducibly bind or do not bind p65.
C. RNA levels (derived from RNA-seq) of hnRNPA1 in primary resting B cells.
D. Protein levels of hnRNPA1 in primary resting B cells.

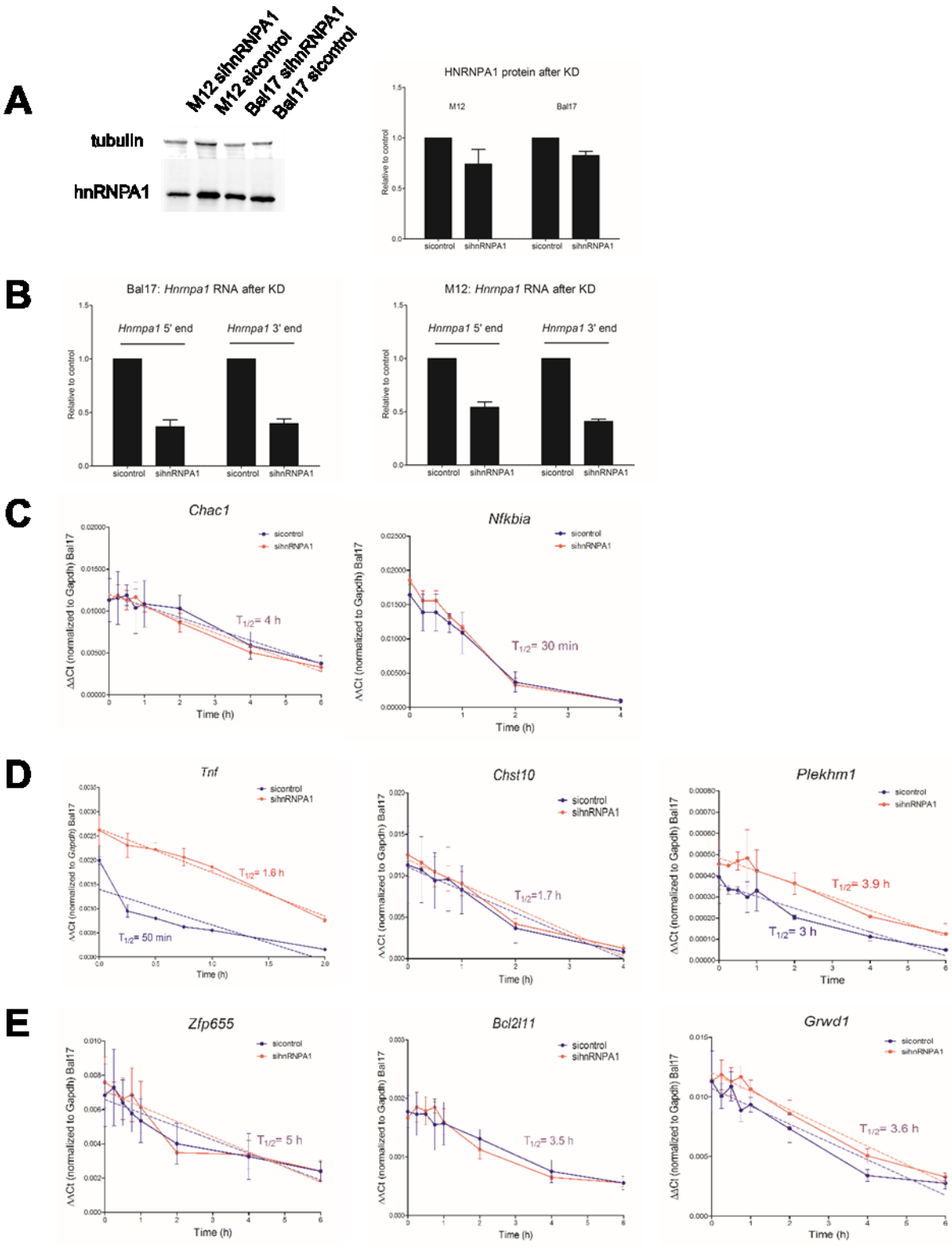

Figure 22. hnRNPA1, at least in part, mediates rapid decay kinetics of BCR-inducible genes.

Figure 22. hnRNPA1, at least in part, mediates rapid decay kinetics of BCR-inducible genes.

A. Protein levels of hnRNPA1 after siRNA-hnRNPA1 knockdown in two B cell lines, Bal17 and M12. Western blot quantitation on right (n=2).
B. RNA levels of hnRNPA1 after siRNA-hnRNPA1 knockdown in two B cell lines, Bal17 and M12.
C. Representative RNA kinetic profiles of genes that do not have hnRNPA1 binding motifs in the 3' UTR with and without hnRNPA1 knockdown.
D. Representative RNA kinetic profiles of genes with hnRNPA1 binding motifs in the 3' UTR and p65-dependent with and without hnRNPA1 knockdown.
E. Representative RNA kinetic profiles of genes without hnRNPA1 binding motifs in the 3' UTR and p65-independent with and without hnRNPA1 knockdown.

Discussion and Conclusion

RelA is a ubiquitous transcription factor and has both specific and unique functions in virtually all cell types. Our study sought to dissect RelA-dependent gene expression in B lymphocytes to gain a global perspective of B cell biology. We used various high-throughput technologies to ultimately link inducible RelA binding to mRNA levels in activated B lymphocytes, both at the level of transcription and mRNA decay. Using RelA ChIP-seq to identify global RelA binding patterns at 0,1, and 4 hours after BCR stimulation in primary B cells, we focused on genes that demonstrate inducible binding within the first hour of activation. Of these genes, most iRelA binding occurred at accessible regions of chromatin (DHS sites at basal state). However, this is likely to be a directed, and not coincidental, process as the most highly enriched motif under the RelA peaks of the genes that demonstrate inducible promoter binding was the consensus NF-κB motif.

Several studies, including our own, have demonstrated that RelA binds relatively promiscuously to accessible parts of the genome, but likely only leads to functional output (RNA) in the presence of cell- and stimulus- specific coactivators. Indeed, we and others have shown that a large number of both constitutive and inducible RelA peaks are present in various cell types and across different stimuli, but only a subset of those genes give rise to RNA. B cells stimulated through the antigen receptor results in genome-wide iRelA binding across promoters, gene bodies, and intergenic regions, with the highest number of genes demonstrating promoter binding. Of these inducible peaks, only a small subset of genes (<40%) result in increased RNA. Most, but not all, productive genes with iRelA binding in the promoter regions were also positive for

H3K4me3 marks and poised PolII. Interestingly, there are a significant fraction of genes with iRelA promoter binding, H3K4me3, and poised PolII, yet do not lead to productive RNA. Motif analyses of promoter regions of genes with and without productive RNA revealed an enrichment of NF-κB/p65 and Usf2, respectively. Thus, it is conceivable that Usf2 is necessary for the expression of non-productive genes, but may not be expressed in B cells or be induced in response to αIgM.

As with most TFs, the activity of RelA is often contingent upon the cooperation between multiple TFs that allows for transcriptional control. In macrophages, for example, RelA binding is largely dependent on PU.1 for binding to newly formed activation-induced enhancers and the subsequent modulation of gene expression [33]. Apart from cell-specific TFs that contribute to RelA activity, stimulus-specific TFs also dictate the response of a cell to an activating stimulus. Our analyses comparing the transcriptomes of BCR- and TLR4- stimulated cells revealed unique subsets of genes that are induced in response to one stimulus, but not the other. Thus, it is likely that only in combination with stimulus-specific TFs, such as MEF2C or IRF4/8 in BCR-stimulated, or EBF1 in LPS-stimulated, B cells, will RelA binding lead to gene expression (**Fig 23**).

One caveat of this study and others like it is the inherent limitation in defining genomic regions in the analysis of the RelA ChIP-seq, which may lead to an inaccurate estimation and/or identification of RelA dependent genes. Our analysis defined the promoter as -3 kb to +1 kb relative to the TSS, which is arbitrary and may be an underestimation in some cases, and an overestimation in others. Even more arbitrarily, the intergenic regions are scored as those that are neither promoter nor genic bodies, and the gene associated with an intergenic peak is that which is the most proximal to

the peak. While this strategy is logically sound, it discounts genes that are RelA dependent in a distal enhancer manner, such as *Ccl3* and *Ccl4*. Despite this, however, this study was rigorous in data analysis and therefore offers reliable insights into RelA biology in activated B cells.

A major goal of this study was to identify ReA target genes in B cells stimulated through the BCR. To do this, we looked to genes that are expressed at least 1.5-fold in activated B cells at 1 hour, demonstrate iRelA binding within the first hour of activation, the peak time of nuclear RelA levels, and coupled this with genes whose expression is robustly downregulated with the treatment of two different NF-κB inhibitors. This strategy revealed approximately 140 genes that are RelA-dependent in B cells stimulated through the BCR. We are also interested in reinforcing these genes as RelA targets using genetic ablation of RelA in primary B cells; preliminary analyses of this method are consistent with the IKK-2 inhibition.

To better understand the complete life cycle of RelA target genes, we performed microarray on ActD treated activated B cells and determined decay rates and half-lives of approximately 1,600 genes. We found that most genes in activated B cells demonstrate long half-lives (>6 hours), consistent with what has previously been reported in primary human T cells [110]. There are approximately 130 genes that with short half-lives (<70 min), which are highly enriched for cytokine production and cytokine biosynthesis, which indicates that pro-inflammatory factors are rapidly synthesized (in a RelA-dependent manner) and subsequently rapidly degraded.

Our results suggest that RelA, which strongly induced transcription of genes that must be tightly regulated (such as inflammatory mediators), is also involved in their rapid

decay in cooperation with decay factors, such as RNABPs. Using CIS-BP, we found an enrichment for hnRNPA1 binding motifs in the 3' UTRs of genes that demonstrate fast, exponential decay in primary B cells. hnRNPA1 has been best studied in the context of alternative splicing as it was originally identified as a switch for splice site selection in adenovirus E1A pre-mRNAs [114]. More recently, however, there is increasing evidence of a role for hnRNPA1 in the regulation of RNA stability. After knockdown of hnRNPA1 in two different B lymphoma cell lines, mRNA of genes with iRelA binding and hnRNPA1 binding sites in the 3' UTR had longer half-lives, while those with hnRNPA1 binding sites but no iRelA binding were largely unaffected. These results offer support of a system based on an hnRNPA1-dependent decay mechanism of RelA dependent transcripts. It has been previously reported that splicing of transcripts in fibroblasts stimulated with TNF regulates the temporal order of genes [58]. It is conceivable, therefore, that hnRNPA1 regulates mRNA stability via splicing, but this warrants further investigation.

Taken together, we identified RelA target genes in primary αIgM stimulated B cells and found that RelA target genes with short half-lives were dependent on the TF for its induction and potentially for its decay (**Fig 23**). Follow-up studies are needed to confirm the role of RelA in hnRNPA1-mediated mRNA decay, which can be done via co-IP experiments. Additionally, target genes that were identified in this study should be further investigated with mutational analyses of NF-κB binding motifs to incontrovertibly prove dependency on RelA. Exploration and elucidation of TF biology is a complicated endeavor, but we believe our stringent approaches and analyses have contributed considerable insight into the roles of RelA in primary activated B cells.

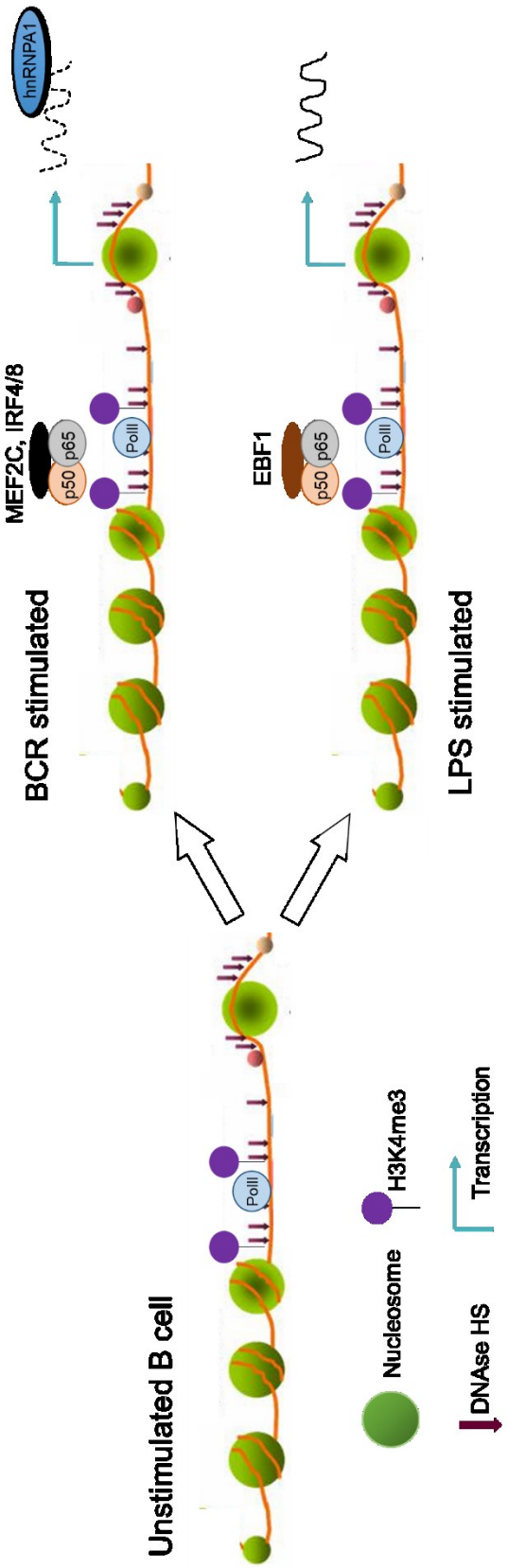

Figure 23. BCR-induced response o

Materials and Methods

Mice

All experimental mice were 8–12 weeks old and on a C57BL/6J background (wild type, WT). Mice were treated humanely in accordance with federal government guidelines and their use was approved by the respective institutional animal care and use committees.

Isolation of B cells and cell culture

Primary B lymphocytes were isolated using RoboSep (StemCell Technologies) magnetic purification techniques by negative selection. B cell purity was 90-95% based on flow cytometric analysis with CD19 staining. Purified B cells ($2x10^6$/ml) were cultured in RPMI 1640 supplemented with 10% heat-inactivated FBS, 55nM β-mercaptoethanol, 2mM L-glutamine and 100IU penicillin and 100µg/ml streptomycin at 37°C. Cells were rested for 45 minutes followed by stimulation with 10 µg/ml goat anti-mouse IgM $F(ab')_2$ (Jackson ImmunoResearch Laboratories). For inhibitor experiments, B cells were pre-treated with

RNA Isolation and Real-Time PCR

RNA Extraction was performed using either Trizol or RNEasy Micro Kits (Qiagen) and qPCR was performed using iTaq Universal SYBR® Green Supermix (Bio-Rad). Primers were designed based on exon-exon junction coverage, ~50% GC content, and 70-150 bp amplicon; primer sequences provided below. qPCR was run using 96 or 384-well plates on the Applied Biosystems 7500 Fast or ViiA7 instrument.

RNA-seq library preparation

cDNA libraries were single-end sequenced (50 bp) on an Illumina HiSeq 2000. Reads were aligned to the mouse genome (NCBI37/mm9 build) with TopHat v1.3.3 and allowing reads to be aligned once with up to two mismatches per read. RPKM values were calculated using Cufflinks 2.2.0, which divides all mapped exonic reads by the length of the spliced product. All RPKM values represent an average of two biological replicates. Only genes that had a minimum RPKM value of 1.5 at any time point across the six-hour time course were included in our analyses. K-means clustering was done using Cluster 3 with log2 normalized RPKM values.

Tat-Cre Treatment

Tat-Cre purified protein (kindly provided by M. Atchison, UPenn) was diluted in warm Opti-MEM and mixed with B cells for a final concentration of 10^7 cells/2ml/100 ug Tat-Cre. Cells were incubated in the presence of Tat-Cre at 37C for 45 minutes after which FBS was added at a final concentration of 10% to stop the reaction. Cells were spun down at 1400rpm for 10 minutes at 4C, washed with warm complete RPMI, counted, and left for 48 hours at 37C. Prior to activation with anti-IgM, dead cells were removed using MicroBead based selection (MACS).

Determination of half-lives

(Modified from Sharova et al)

We set a minimum threshold of 150 (raw intensity value) from the Affymetrix Microarray. Using RNA treated with IgM and Actinomycin D, a transcript was defined as increasing if the slope between two consecutive time points had a positive value and decreasing if the slope had a negative value. We looked only to those genes that demonstrated peak

RNA levels at either one or two hours after IgM stimulation (coinciding with peak nuclear levels of RelA) and ActD treatment. From the peak expression time to the time at which RNA levels stopped decreasing (based on slope), the points of RNA decline were fitted to a line and deemed exponential if the slope was ≥0.9 and nonexponential if the slope was <0.9. Degradation rates of mRNA were estimated using linear regression of base 10 log transformed signal intensity values (y) versus time (t): $y=a-bt$, where b is the slope and a is the y-intercept. The instantaneous decay rate (d) was determined by the equation $d= b*\ln(10)$. For probes that leveled off early in the six hour time course (i.e. those with fast decay), we manually truncated the later time points. Following application of these criteria, half-lives (H) of genes with exponential decay were determined using the equation $H=\min(24,\ln(2)/d)$.

Primer Sequences

GAPDH F	TCAACAGCAACTCCCACTCTTCCA
GAPDH R	ACCCTGTTGCTGTAGCCGTATTCA
CCL3 F	TTTGAAACCAGCAGCCTTTGCTCC
CCL3 R	TCAGGCATTCAGTTCCAGGTCAGT
CCL4 F	ATGAGACCAGCAGTCTTTGCTCCA
CCL4 R	GCTGCTCAGTTCAACTCCAAGTCA
NFKBIA F	TCTGAAAGCTGGCTGTGATCCTGA
NFKBIA R	AGACACGTGTGGCCATTGTAGTTG
TNF F	AATGGCCTCCTCTCATCAGTTCT
TNF R	GGTTGTCTTTGAGATCCATGCCGT
IRF4 F	GAGCTGCAAGTGTTTGCTCACCAT
IRF4 R	ACAGTTGTCTGGCTAGCAGAGGTT
MYC F	ATTTCCTTTGGGCGTTGGAAACCC
MYC R	TCGTCGCAGATGAAATAGGGCTGT
TNFAIP3 F	TCAACTGGTGTCGTGAAGTCAGGA
TNFAIP3 R	AGGACCAGGTCAGTATCCTGAACA
VEGFA F	CTTCCTACAGCACAGCAGATGTGA
VEGFA R	ACCGGGATTTCTTGCGCTTTCGTTT
NR4A1 F	TGACAATTCGTGTCAGCAC
NR4A1 R	ACAGGGCAATCCTTGTTTGCCA

References

1. Sen, R. and D. Baltimore, *Inducibility of kappa immunoglobulin enhancer-binding protein Nf-kappa B by a posttranslational mechanism.* Cell, 1986. **47**(6): p. 921-8.
2. Hayden, M.S. and S. Ghosh, *NF-kappaB, the first quarter-century: remarkable progress and outstanding questions.* Genes Dev, 2012. **26**(3): p. 203-34.
3. Cildir, G., K.C. Low, and V. Tergaonkar, *Noncanonical NF-kappaB Signaling in Health and Disease.* Trends Mol Med, 2016. **22**(5): p. 414-29.
4. Latimer, M., et al., *The N-terminal domain of IkappaB alpha masks the nuclear localization signal(s) of p50 and c-Rel homodimers.* Mol Cell Biol, 1998. **18**(5): p. 2640-9.
5. Gerondakis, S., et al., *Genetic approaches in mice to understand Rel/NF-kappaB and IkappaB function: transgenics and knockouts.* Oncogene, 1999. **18**(49): p. 6888-95.
6. Jurk, D., et al., *Chronic inflammation induces telomere dysfunction and accelerates ageing in mice.* Nat Commun, 2014. **2**: p. 4172.
7. Hayden, M.S. and S. Ghosh, *Shared principles in NF-kappaB signaling.* Cell, 2008. **132**(3): p. 344-62.
8. Stadanlick, J.E., et al., *Tonic B cell antigen receptor signals supply an NF-kappaB substrate for prosurvival BLyS signaling.* Nat Immunol, 2008. **9**(12): p. 1379-87.
9. Legarda-Addison, D. and A.T. Ting, *Negative regulation of TCR signaling by NF-kappaB2/p100.* J Immunol, 2007. **178**(12): p. 7767-78.
10. de Wit, H., et al., *Regulation of p100 (NFKB2) expression in human monocytes in response to inflammatory mediators and lymphokines.* Leukemia, 1998. **12**(3): p. 363-70.
11. Shih, V.F., et al., *A single NFkappaB system for both canonical and non-canonical signaling.* Cell Res, 2011. **21**(1): p. 86-102.
12. Spina, V. and D. Rossi, *NF-kappaB deregulation in splenic marginal zone lymphoma.* Semin Cancer Biol, 2016. **39**: p. 61-7.
13. Karin, M., *NF-kappaB as a critical link between inflammation and cancer.* Cold Spring Harb Perspect Biol, 2009. **1**(5): p. a000141.
14. Xia, Y., S. Shen, and I.M. Verma, *NF-kappaB, an active player in human cancers.* Cancer Immunol Res, 2014. **2**(9): p. 823-30.
15. Bektas, A., et al., *Age-associated changes in basal NF-kappaB function in human CD4+ T lymphocytes via dysregulation of PI3 kinase.* Aging (Albany NY), 2014. **6**(11): p. 957-74.
16. Tilstra, J.S., et al., *NF-kappaB in Aging and Disease.* Aging Dis, 2011. **2**(6): p. 449-65.
17. Salminen, A., et al., *Activation of innate immunity system during aging: NF-kB signaling is the molecular culprit of inflamm-aging.* Ageing Res Rev, 2008. **7**(2): p. 83-105.
18. Sen, R. and S.T. Smale, *Selectivity of the NF-{kappa}B response.* Cold Spring Harb Perspect Biol, 2010. **2**(4): p. a000257.
19. Pahl, H.L., *Activators and target genes of Rel/NF-kappaB transcription factors.* Oncogene, 1999. **18**(49): p. 6853-66.

20. Oeckinghaus, A. and S. Ghosh, *The NF-kappaB family of transcription factors and its regulation.* Cold Spring Harb Perspect Biol, 2009. **1**(4): p. a000034.
21. Lim, C.A., et al., *Genome-wide mapping of RELA(p65) binding identifies E2F1 as a transcriptional activator recruited by NF-kappaB upon TLR4 activation.* Mol Cell, 2007. **27**(4): p. 622-35.
22. Barish, G.D., et al., *Bcl-6 and NF-kappaB cistromes mediate opposing regulation of the innate immune response.* Genes Dev, 2010. **24**(24): p. 2760-5.
23. Schreiber, J., et al., *Coordinated binding of NF-kappaB family members in the response of human cells to lipopolysaccharide.* Proc Natl Acad Sci U S A, 2006. **103**(15): p. 5899-904.
24. Ghosh, G., et al., *Structure of NF-kappa B p50 homodimer bound to a kappa B site.* Nature, 1995. **373**(6512): p. 303-10.
25. Muller, C.W., et al., *Structure of the NF-kappa B p50 homodimer bound to DNA.* Nature, 1995. **373**(6512): p. 311-7.
26. Chen, F.E., et al., *Crystal structure of p50/p65 heterodimer of transcription factor NF-kappaB bound to DNA.* Nature, 1998. **391**(6665): p. 410-3.
27. Muroi, M., et al., *Influence of 3' half-site sequence of NF-kappa B motifs on the binding of lipopolysaccharide-activatable macrophage NF-kappa B proteins.* J Biol Chem, 1993. **268**(26): p. 19534-9.
28. Schreck, R., et al., *The NF-kappa B transcription factor induces DNA bending which is modulated by its 65-kD subunit.* Nucleic Acids Res, 1990. **18**(22): p. 6497-502.
29. Wang, V.Y., et al., *The transcriptional specificity of NF-kappaB dimers is coded within the kappaB DNA response elements.* Cell Rep, 2012. **2**(4): p. 824-39.
30. Leung, T.H., A. Hoffmann, and D. Baltimore, *One nucleotide in a kappaB site can determine cofactor specificity for NF-kappaB dimers.* Cell, 2004. **118**(4): p. 453-64.
31. John, S., et al., *Chromatin accessibility pre-determines glucocorticoid receptor binding patterns.* Nat Genet, 2011. **43**(3): p. 264-8.
32. Carroll, J.S., et al., *Genome-wide analysis of estrogen receptor binding sites.* Nat Genet, 2006. **38**(11): p. 1289-97.
33. Kaikkonen, M.U., et al., *Remodeling of the enhancer landscape during macrophage activation is coupled to enhancer transcription.* Mol Cell, 2013. **51**(3): p. 310-25.
34. Papantonis, A., et al., *TNFalpha signals through specialized factories where responsive coding and miRNA genes are transcribed.* EMBO J, 2012. **31**(23): p. 4404-14.
35. Kuznetsova, T., et al., *Glucocorticoid receptor and nuclear factor kappa-b affect three-dimensional chromatin organization.* Genome Biol, 2015. **16**: p. 264.
36. Martone, R., et al., *Distribution of NF-kappaB-binding sites across human chromosome 22.* Proc Natl Acad Sci U S A, 2003. **100**(21): p. 12247-52.
37. Cieslik, M. and S. Bekiranov, *Genome-wide predictors of NF-kappaB recruitment and transcriptional activity.* BioData Min, 2015. **8**: p. 37.
38. Siggers, T., et al., *Principles of dimer-specific gene regulation revealed by a comprehensive characterization of NF-kappaB family DNA binding.* Nat Immunol, 2011. **13**(1): p. 95-102.

39. Tong, A.J., et al., *A Stringent Systems Approach Uncovers Gene-Specific Mechanisms Regulating Inflammation.* Cell, 2016. **165**(1): p. 165-79.
40. Jin, F., et al., *PU.1 and C/EBP(alpha) synergistically program distinct response to NF-kappaB activation through establishing monocyte specific enhancers.* Proc Natl Acad Sci U S A, 2011. **108**(13): p. 5290-5.
41. Song, L., et al., *Open chromatin defined by DNaseI and FAIRE identifies regulatory elements that shape cell-type identity.* Genome Res, 2011. **21**(10): p. 1757-67.
42. Thurman, R.E., et al., *The accessible chromatin landscape of the human genome.* Nature, 2012. **489**(7414): p. 75-82.
43. Boyes, J. and G. Felsenfeld, *Tissue-specific factors additively increase the probability of the all-or-none formation of a hypersensitive site.* EMBO J, 1996. **15**(10): p. 2496-507.
44. Rao, N.A., et al., *Coactivation of GR and NFKB alters the repertoire of their binding sites and target genes.* Genome Res, 2011. **21**(9): p. 1404-16.
45. Raskatov, J.A., et al., *Modulation of NF-kappaB-dependent gene transcription using programmable DNA minor groove binders.* Proc Natl Acad Sci U S A, 2012. **109**(4): p. 1023-8.
46. Diermeier, S., et al., *TNFalpha signalling primes chromatin for NF-kappaB binding and induces rapid and widespread nucleosome repositioning.* Genome Biol, 2014. **15**(12): p. 536.
47. Mukherjee, S.P., et al., *Analysis of the RelA:CBP/p300 interaction reveals its involvement in NF-kappaB-driven transcription.* PLoS Biol, 2013. **11**(9): p. e1001647.
48. Dong, J., et al., *Repression of gene expression by unphosphorylated NF-kappaB p65 through epigenetic mechanisms.* Genes Dev, 2008. **22**(9): p. 1159-73.
49. Sanjabi, S., et al., *A c-Rel subdomain responsible for enhanced DNA-binding affinity and selective gene activation.* Genes Dev, 2005. **19**(18): p. 2138-51.
50. Zhou, A., et al., *Identification of NF-kappa B-regulated genes induced by TNFalpha utilizing expression profiling and RNA interference.* Oncogene, 2003. **22**(13): p. 2054-64.
51. Tian, B., et al., *Identification of direct genomic targets downstream of the nuclear factor-kappaB transcription factor mediating tumor necrosis factor signaling.* J Biol Chem, 2005. **280**(17): p. 17435-48.
52. Nelson, D.E., et al., *Oscillations in NF-kappaB signaling control the dynamics of gene expression.* Science, 2004. **306**(5696): p. 704-8.
53. Lee, R.E., et al., *Fold change of nuclear NF-kappaB determines TNF-induced transcription in single cells.* Mol Cell, 2014. **53**(6): p. 867-79.
54. Sung, M.H., et al., *Sustained oscillations of NF-kappaB produce distinct genome scanning and gene expression profiles.* PLoS One, 2009. **4**(9): p. e7163.
55. Nelson, G., et al., *Multi-parameter analysis of the kinetics of NF-kappaB signalling and transcription in single living cells.* J Cell Sci, 2002. **115**(Pt 6): p. 1137-48.
56. Core, L.J., et al., *Analysis of nascent RNA identifies a unified architecture of initiation regions at mammalian promoters and enhancers.* Nat Genet, 2014. **46**(12): p. 1311-20.

57. Bhatt, D. and S. Ghosh, *Regulation of the NF-kappaB-Mediated Transcription of Inflammatory Genes.* Front Immunol, 2014. **5**: p. 71.
58. Hao, S. and D. Baltimore, *RNA splicing regulates the temporal order of TNF-induced gene expression.* Proceedings of the National Academy of Sciences, 2013. **110**(29): p. 11934-11939.
59. Zambrano, S., et al., *NF-kappaB oscillations translate into functionally related patterns of gene expression.* Elife, 2016. **5**: p. e09100.
60. Hao, S. and D. Baltimore, *The stability of mRNA influences the temporal order of the induction of genes encoding inflammatory molecules.* Nat Immunol, 2009. **10**(3): p. 281-8.
61. Bhatt, D.M., et al., *Transcript dynamics of proinflammatory genes revealed by sequence analysis of subcellular RNA fractions.* Cell, 2012. **150**(2): p. 279-90.
62. Yu, J., A.G. Freud, and M.A. Caligiuri, *Location and cellular stages of natural killer cell development.* Trends Immunol, 2013. **34**(12): p. 573-82.
63. Pillai, S. and A. Cariappa, *The follicular versus marginal zone B lymphocyte cell fate decision.* Nat Rev Immunol, 2009. **9**(11): p. 767-77.
64. Barwick, B.G., et al., *Plasma cell differentiation is coupled to division-dependent DNA hypomethylation and gene regulation.* Nat Immunol, 2016. **17**(10): p. 1216-25.
65. Fowler, T., et al., *Divergence of transcriptional landscape occurs early in B cell activation.* Epigenetics Chromatin, 2015. **8**: p. 20.
66. Gerondakis, S. and U. Siebenlist, *Roles of the NF-kappaB pathway in lymphocyte development and function.* Cold Spring Harb Perspect Biol, 2010. **2**(5): p. a000182.
67. Kaileh, M. and R. Sen, *NF-kappaB function in B lymphocytes.* Immunol Rev, 2012. **246**(1): p. 254-71.
68. Schiemann, B., et al., *An essential role for BAFF in the normal development of B cells through a BCMA-independent pathway.* Science, 2001. **293**(5537): p. 2111-4.
69. Thompson, J.S., et al., *BAFF-R, a newly identified TNF receptor that specifically interacts with BAFF.* Science, 2001. **293**(5537): p. 2108-11.
70. Kraus, M., et al., *Survival of resting mature B lymphocytes depends on BCR signaling via the Igalpha/beta heterodimer.* Cell, 2004. **117**(6): p. 787-800.
71. Lam, K.P., R. Kuhn, and K. Rajewsky, *In vivo ablation of surface immunoglobulin on mature B cells by inducible gene targeting results in rapid cell death.* Cell, 1997. **90**(6): p. 1073-83.
72. Li, Z.W., et al., *IKK beta is required for peripheral B cell survival and proliferation.* J Immunol, 2003. **170**(9): p. 4630-7.
73. Pasparakis, M., M. Schmidt-Supprian, and K. Rajewsky, *IkappaB kinase signaling is essential for maintenance of mature B cells.* J Exp Med, 2002. **196**(6): p. 743-52.
74. Kaisho, T., et al., *IkappaB kinase alpha is essential for mature B cell development and function.* J Exp Med, 2001. **193**(4): p. 417-26.
75. Senftleben, U., et al., *Activation by IKKalpha of a second, evolutionary conserved, NF-kappa B signaling pathway.* Science, 2001. **293**(5534): p. 1495-9.

76. Damdinsuren, B., et al., *Single round of antigen receptor signaling programs naive B cells to receive T cell help.* Immunity, 2010. **32**(3): p. 355-66.
77. Owyang, A.M., et al., *c-Rel is required for the protection of B cells from antigen receptor-mediated, but not Fas-mediated, apoptosis.* J Immunol, 2001. **167**(9): p. 4948-56.
78. Kontgen, F., et al., *Mice lacking the c-rel proto-oncogene exhibit defects in lymphocyte proliferation, humoral immunity, and interleukin-2 expression.* Genes Dev, 1995. **9**(16): p. 1965-77.
79. Opata, M.M., et al., *B cell production of tumor necrosis factor in response to Pneumocystis murina infection in mice.* Infect Immun, 2013. **81**(11): p. 4252-60.
80. Schall, T.J., et al., *Human macrophage inflammatory protein alpha (MIP-1 alpha) and MIP-1 beta chemokines attract distinct populations of lymphocytes.* J Exp Med, 1993. **177**(6): p. 1821-6.
81. Venkataraman, L., et al., *Cyclosporin-A sensitive induction of NF-AT in murine B cells.* Immunity, 1994. **1**(3): p. 189-96.
82. Choi, M.S., et al., *Induction of NF-AT in normal B lymphocytes by anti-immunoglobulin or CD40 ligand in conjunction with IL-4.* Immunity, 1994. **1**(3): p. 179-87.
83. Gross, D.S. and W.T. Garrard, *Nuclease hypersensitive sites in chromatin.* Annu Rev Biochem, 1988. **57**: p. 159-97.
84. Wu, C., Y.C. Wong, and S.C. Elgin, *The chromatin structure of specific genes: II. Disruption of chromatin structure during gene activity.* Cell, 1979. **16**(4): p. 807-14.
85. Meyer, C.A. and X.S. Liu, *Identifying and mitigating bias in next-generation sequencing methods for chromatin biology.* Nat Rev Genet, 2014. **15**(11): p. 709-21.
86. Barski, A., et al., *High-resolution profiling of histone methylations in the human genome.* Cell, 2007. **129**(4): p. 823-37.
87. Zhao, B., et al., *The NF-kappaB genomic landscape in lymphoblastoid B cells.* Cell Rep, 2014. **8**(5): p. 1595-606.
88. Bannister, A.J., et al., *Spatial distribution of di- and tri-methyl lysine 36 of histone H3 at active genes.* J Biol Chem, 2005. **280**(18): p. 17732-6.
89. Peters, A.H., et al., *Partitioning and plasticity of repressive histone methylation states in mammalian chromatin.* Mol Cell, 2003. **12**(6): p. 1577-89.
90. Pierce, J.W., et al., *Novel inhibitors of cytokine-induced IkappaBalpha phosphorylation and endothelial cell adhesion molecule expression show anti-inflammatory effects in vivo.* J Biol Chem, 1997. **272**(34): p. 21096-103.
91. Podolin, P.L., et al., *Attenuation of murine collagen-induced arthritis by a novel, potent, selective small molecule inhibitor of IkappaB Kinase 2, TPCA-1 (2-[(aminocarbonyl)amino]-5-(4-fluorophenyl)-3-thiophenecarboxamide), occurs via reduction of proinflammatory cytokines and antigen-induced T cell Proliferation.* J Pharmacol Exp Ther, 2005. **312**(1): p. 373-81.
92. Grove, M. and M. Plumb, *C/EBP, NF-kappa B, and c-Ets family members and transcriptional regulation of the cell-specific and inducible macrophage inflammatory protein 1 alpha immediate-early gene.* Mol Cell Biol, 1993. **13**(9): p. 5276-89.

93. Rabani, M., et al., *Metabolic labeling of RNA uncovers principles of RNA production and degradation dynamics in mammalian cells.* Nat Biotechnol, 2011. **29**(5): p. 436-42.
94. Paulsen, M.T., et al., *Coordinated regulation of synthesis and stability of RNA during the acute TNF-induced proinflammatory response.* Proc Natl Acad Sci U S A, 2013. **110**(6): p. 2240-5.
95. Kuersten, S. and E.B. Goodwin, *The power of the 3' UTR: translational control and development.* Nat Rev Genet, 2003. **4**(8): p. 626-37.
96. Ivanov, P. and P. Anderson, *Post-transcriptional regulatory networks in immunity.* Immunol Rev, 2013. **253**(1): p. 253-72.
97. Beisang, D. and P.R. Bohjanen, *Perspectives on the ARE as it turns 25 years old.* Wiley Interdiscip Rev RNA, 2012. **3**(5): p. 719-31.
98. Moraes, K.C., C.J. Wilusz, and J. Wilusz, *CUG-BP binds to RNA substrates and recruits PARN deadenylase.* RNA, 2006. **12**(6): p. 1084-91.
99. Pautz, A., et al., *The polypyrimidine tract-binding protein (PTB) is involved in the post-transcriptional regulation of human inducible nitric oxide synthase expression.* J Biol Chem, 2006. **281**(43): p. 32294-302.
100. Early, P., et al., *Two mRNAs can be produced from a single immunoglobulin mu gene by alternative RNA processing pathways.* Cell, 1980. **20**(2): p. 313-9.
101. Rogers, J., et al., *Two mRNAs with different 3' ends encode membrane-bound and secreted forms of immunoglobulin mu chain.* Cell, 1980. **20**(2): p. 303-12.
102. Alt, F.W., et al., *Synthesis of secreted and membrane-bound immunoglobulin mu heavy chains is directed by mRNAs that differ at their 3' ends.* Cell, 1980. **20**(2): p. 293-301.
103. Di Giammartino, D.C., K. Nishida, and J.L. Manley, *Mechanisms and consequences of alternative polyadenylation.* Mol Cell, 2011. **43**(6): p. 853-66.
104. Sharova, L.V., et al., *Database for mRNA half-life of 19 977 genes obtained by DNA microarray analysis of pluripotent and differentiating mouse embryonic stem cells.* DNA Res, 2009. **16**(1): p. 45-58.
105. Friedel, C.C., et al., *Conserved principles of mammalian transcriptional regulation revealed by RNA half-life.* Nucleic Acids Res, 2009. **37**(17): p. e115.
106. Bregman, A., et al., *Promoter elements regulate cytoplasmic mRNA decay.* Cell, 2011. **147**(7): p. 1473-83.
107. Haimovich, G., et al., *Gene expression is circular: factors for mRNA degradation also foster mRNA synthesis.* Cell, 2013. **153**(5): p. 1000-11.
108. Rambout, X., et al., *The transcription factor ERG recruits CCR4-NOT to control mRNA decay and mitotic progression.* Nat Struct Mol Biol, 2016. **23**(7): p. 663-72.
109. Carpenter, S., et al., *Post-transcriptional regulation of gene expression in innate immunity.* Nat Rev Immunol, 2014. **14**(6): p. 361-76.
110. Raghavan, A., et al., *Genome-wide analysis of mRNA decay in resting and activated primary human T lymphocytes.* Nucleic Acids Res, 2002. **30**(24): p. 5529-38.
111. Xia, Z., et al., *Dynamic analyses of alternative polyadenylation from RNA-seq reveal a 3'-UTR landscape across seven tumour types.* Nat Commun, 2014. **5**: p. 5274.

112. Geissler, R., et al., *A widespread sequence-specific mRNA decay pathway mediated by hnRNPs A1 and A2/B1.* Genes Dev, 2016. **30**(9): p. 1070-85.
113. Wang, H., et al., *hnRNP A1 antagonizes cellular senescence and senescence-associated secretory phenotype via regulation of SIRT1 mRNA stability.* Aging Cell, 2016.
114. Mayeda, A. and A.R. Krainer, *Regulation of alternative pre-mRNA splicing by hnRNP A1 and splicing factor SF2.* Cell, 1992. **68**(2): p. 365-75.

The Johns Hopkins School of Medicine

Jaimy P. Joy June 6, 2017

Educational history:

Ph.D. expected	2017	Program in Immunology Mentor: Ranjan Sen, Ph.D.	Johns Hopkins School of Medicine
B.S.	2011	Biology	The Pennsylvania State University
B.S.	2011	Immunology	The Pennsylvania State University
B.S.	2011	Toxicology	The Pennsylvania State University

Other professional experience

Summer Internship	2010	Lab of Luc Teyton, Ph.D., The Scripps Research Institute
Student Researcher	2007-2011	Lab of Joe Reese, PhD The Pennsylvania State University
Student Researcher	2006-2007	Lab of Dr. Carlo Maley, Wistar Institute
Student Scientist	2004-2006	Lab of Dr. Glenn Rall, Fox Chase Cancer Center

Funding and support

National Institutes of Health Pre-Doctoral IRTA Fellowship 2012-1017

Academic awards and honors

2016 NIA Director's Award for Scientific Excellence NIA

Publications

Armistead J, Morlais I, Matthias D, Jardim J, **Joy J**, Fridman A, Finnefrock A, Churcher T, Scorpio D, Borg N, Sattabongkot J, and Dinglasan R. Progress towards a pan-malaria transmission-blocking vaccine. *Infection and Immunity.* 2013.

Posters and abstracts

Joy J, Kaila M, and Sen R. (2014) NF-κB in cellular senescence. Immunology Interest Group Retreat, Bethesda, MD, September 2014.

Joy J, Kaila M, and Sen R. (2015) NF-κB in cellular senescence. Immunology Interest Group Retreat, Bethesda, MD, September 2015.

Joy J, Zhao M, Hao H, Wood WH, De S, Becker K, and Sen R. (2014) Post-transcriptional regulation of NF-κB in primary B lymphocytes. NIH Graduate Student Symposium, Bethesda, MD, January 2014.

Joy J, Zhao M, Hao H, Wood WH, De S, Becker K, and Sen R. (2015) Post-transcriptional regulation of NF-κB in primary B lymphocytes. NIH Graduate Student Symposium, Bethesda, MD, January 2015.

Joy J, Zhao M, Hao H, Wood WH, De S, Becker K, and Sen R. (2016) Post-transcriptional regulation of NF-κB in primary B lymphocytes. NIH Graduate Student Symposium, Bethesda, MD, January 2016.

Joy J, Kaila M, and Sen R. (2014) NF-κB in cellular senescence. NIA/NIDA Research Symposium, Baltimore, MD, September 2014.

Joy J, Kaila M, and Sen R. (2015) NF-κB in cellular senescence. NIA/NIDA Research Symposium, Baltimore, MD, September 2015.

Joy J, Kaila M, and Sen R. (2015) NF-κB in cellular senescence. National Institute on Aging Retreat, Bethesda, MD, September 2015.

Joy J, Kaila M, and Sen R. (2016) NF-κB in cellular senescence. National Institute on Aging Retreat, Bethesda, MD, September 2016.

Joy J, Zhao M, Hao H, Wood WH, De S, Becker K, and Sen R. (2016) Post-transcriptional regulation of NF-κB in primary B lymphocytes. Keystone Symposium on Molecular and Cellular Biology: NF-kappaB and MAP Kinase Signaling in Inflammation. Whistler, British Columbia, Canada. March 2016.

Service and leadership

2011-2012	Hand in Hand Baltimore, Mentor
2013-2014	National Commission on Teaching and America's Future (NCTAF)
2014	USA Science and Engineering Festival Volunteer
2014-2016	STEM Achievement in Baltimore Elementary Schools (SABES)
2014-2017	Graduate Student Chronicles Writer and Editor
2015-2016	Campaign Team of Mark Edelson, candidate for Baltimore First District Councilman
2016	Teaching Assistant for Graduate Level Immunology Course